

Extreme value statistics and arcsine laws for heterogeneous diffusion processes

Prashant Singh*

International Centre for Theoretical Sciences, Tata Institute of Fundamental Research, Bengaluru 560089, India

(Dated: December 2, 2021)

Heterogeneous diffusion with spatially changing diffusion coefficient arises in many experimental systems like protein dynamics in the cell cytoplasm, mobility of cajal bodies and confined hard-sphere fluids. Here, we showcase a simple model of heterogeneous diffusion where the diffusion coefficient $D(x)$ varies in power-law way, i.e. $D(x) \sim |x|^{-\alpha}$ with the exponent $\alpha > -1$. This model exhibits anomalous scaling of the mean squared displacement (MSD) of the form $\sim t^{\frac{2}{2+\alpha}}$ and weak ergodicity breaking in the sense that ensemble averaged and time averaged MSDs do not converge. In this paper, we look at the extreme value statistics of this model and derive, for all α , the exact probability distributions of the maximum spatial displacement $M(t)$ and arg-maximum $t_m(t)$ (i.e. the time at which this maximum is reached) till duration t . In the second part of our paper, we analyze the statistical properties of the residence time $t_r(t)$ and the last-passage time $t_\ell(t)$ and compute their distributions exactly for all values of α . Our study unravels that the heterogeneous version ($\alpha \neq 0$) displays many rich and contrasting features compared to that of the standard Brownian motion (SBm). For example, while for SBm ($\alpha = 0$), the distributions of $t_m(t)$, $t_r(t)$ and $t_\ell(t)$ are all identical (*à la* “arcsine laws” due to Lévy), they turn out to be significantly different for non-zero α . Another interesting property of $t_r(t)$ is the existence of a critical α (which we denote by $\alpha_c = -0.3182$) such that the distribution exhibits a local maximum at $t_r = t/2$ for $\alpha < \alpha_c$ whereas it has minima at $t_r = t/2$ for $\alpha \geq \alpha_c$. The underlying reasoning for this difference hints at the very contrasting natures of the process for $\alpha \geq \alpha_c$ and $\alpha < \alpha_c$ which we thoroughly examine in our paper. All our analytical results are backed by extensive numerical simulations.

I. INTRODUCTION

Many real-world systems involve motion of tracer particles in a heterogeneous medium with substantial spatial variations of the diffusion coefficient. For example, in [1, 2], the dynamics of protein in the cell cytoplasm was shown to exhibit a systematic spatial variation of the diffusion coefficient by using mesoscopic numerical methods. Similarly, the mobility of cajal bodies (nuclear organelles) inside living cells develops heterogeneity due to their interactions with other nuclear components [3]. Other examples of heterogeneous diffusion include particle moving between nearly parallel plates [4], diffusion in presence of temperature gradient [5], diffusion in nanoporous solids [6], confined hard sphere fluid [7] and so on. Descriptions with space-dependent diffusion coefficient have also been used in modelling the diffusion in turbulent media [8] and on fractal objects [9]. Several studies on heterogeneous diffusive processes (HDPs) have revealed anomalous scaling of the mean squared displacement (MSD) and weak ergodicity breaking between time averaged and ensemble averaged MSDs [10–16]. Persistent properties of HDPs have also been investigated in [17, 18].

In this paper, we analyse a simple model of one dimensional HDP where the diffusion coefficient has a power-law dependence on the position of the particle, i.e. $D(x) \sim |x|^{-\alpha}$ with $\alpha > -1$. For $\alpha = 0$, it reduces to the homogeneous case of standard Brownian motion (SBm). While the SBm is extensively studied in the literature

and a large number of results are known, the amount of studies for HDPs is far from exhaustive. In an attempt towards this direction, we here investigate the extreme value statistics (EVS) of the HDP with power-law form for $D(x)$. In particular, we study the statistics of the maximum $M(t)$ of the trajectory $x(t)$ observed till time t and the time $t_m(t)$ at which this maximum is achieved. For SBm ($\alpha = 0$), the marginal distributions of $M(t)$ and $t_m(t)$ read [19]

$$P_m(M|t) = \frac{1}{\sqrt{\pi D_0 t}} \exp\left(-\frac{M^2}{4D_0 t}\right), \quad (1)$$

$$P_m(t_m|t) = \frac{1}{\pi \sqrt{t_m(t-t_m)}}, \quad (2)$$

where D_0 is the diffusion coefficient. The study of the extremal statistics has been performed for a variety of stochastic processes like Brownian motion, random walk and their generalisations [19–27], random acceleration [28–30], active particles [31, 32], fractional Brownian motion [33–35], continuous time random walk [36], random matrices [37–39], fluctuating interfaces [40–42], transport models [43–45], finance [46] and other physical systems [47–51] (see [52–61] for review). The subject of EVS has found applications in ecology [62], computer science [63–65] and convex hull problems [66]. Generalising these studies, the statistics of the time between maximum and minimum spatial displacements was also recently considered for Brownian motion and random walks in [67, 68].

Even though there has been a substantial amount of study on EVS, most of these studies, however, are based on homogeneous setup. On the other hand, we saw above that, in many physical systems, the heterogeneous description becomes more relevant. A natural question then

* prashant.singh@icts.res.in

follows - what happens to the distributions of $M(t)$ and $t_m(t)$ in Eqs. (1) and (2) when the dynamics takes place in a heterogeneous medium? Our work aims to provide a systematic understanding to this question in the context of HDPs with power-law form of $D(x)$. Our study demonstrates that the extremal statistics of this model is rather rich and possesses many contrasting features compared to that of the SBm.

In the second part of our paper, we investigate the statistical properties of the following two quantities measured along a trajectory $x(t)$ observed till time t : (i) residence time $t_r(t)$ spent on the positive (or negative) semi axis and (ii) last time $t_\ell(t)$ that the particle crosses the origin. The celebrated *arcsine laws* for one dimensional Brownian motion state that the probability distributions of $t_m(t)$, $t_r(t)$ and $t_\ell(t)$ are all exactly same and given by [19, 69]

$$\mathcal{P}_i(t_i|t) = \frac{1}{\pi\sqrt{t_i(t-t_i)}}, \quad (3)$$

where $t_i \in \{t_m, t_r, t_\ell\}$. The corresponding cumulative probability has the ‘arcsine’ form

$$\text{Prob}[t_i \leq t] = \frac{2}{\pi} \arcsine \left(\sqrt{\frac{t_i}{t}} \right), \quad (4)$$

and hence the name *arcsine laws*. Over the years, these quantities have been studied in different contexts like Brownian motion, random walks and their generalisations [69–76], random acceleration [28, 77], continuous time random walk [36, 78], fractional Brownian motion [34], run and tumble particle [31, 79], finance [46, 80, 81], renewal processes and other processes [82–86]. Quite recently, *arcsine laws* have also been studied both experimentally and theoretically in stochastic thermodynamics [87, 88]. Here, we look at the statistics of $t_r(t)$ and $t_\ell(t)$ in conjunction with $t_m(t)$ for the HDPs with power-law form of $D(x)$. More specifically, our interest is to check whether the universality of these quantities for $\alpha = 0$ gets extended even in presence of heterogeneity. We find that while their distributions are exactly same for $\alpha = 0$ (SBm), they turn out to be significantly different for non-zero α . Our work provides the exact expression of the probability distributions of $M(t)$, $t_m(t)$, $t_r(t)$ and $t_\ell(t)$ for all $\alpha > -1$.

The remainder of paper is structured as follows: We define our model in Sec. II and also present all our main results here. Sec. III presents derivation of the joint distribution of $M(t)$ and $t_m(t)$ which is then used to obtain the marginal distribution of $M(t)$ in Sec. III C and that of $t_m(t)$ in Sec. III D. We next compute the distributions of residence time $t_r(t)$ and last-passage time $t_\ell(t)$ in Secs. IV and V respectively. Finally, we conclude in Sec. VI.

II. MODEL AND SUMMARY OF RESULTS

We study the motion of a particle in one dimension moving in a heterogeneous medium. The heterogeneity is

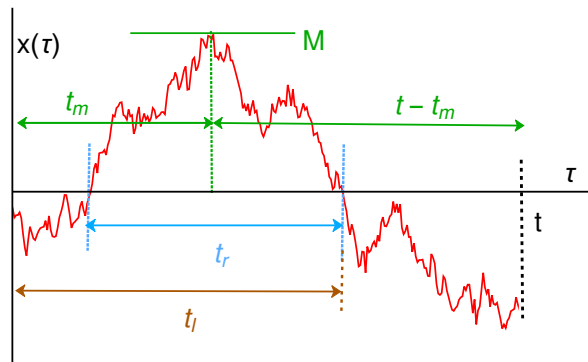


FIG. 1. An schematic illustration of the maximum distance M attained by the process $x(\tau)$ (shown in red) in Eq. (5) till duration t , i.e. $M(t) = \max\{x(\tau)\}$, where $0 \leq \tau \leq t$. The time t_m represents the time at which this maximum is attained. The time t_r represents the amount of time for which $x(\tau)$ stays in the positive semi-axis and the duration t_ℓ is the last time that the process changes its sign (or crosses the origin).

administered by considering the position-dependent diffusion coefficient $D(x)$. The time evolution equation for the position of the particle reads

$$\frac{dx}{dt} = \sqrt{2D(x)} \eta(t), \quad (5)$$

where $\eta(t)$ is the Gaussian white noise with zero mean and correlation $\langle \eta(t)\eta(t') \rangle = \delta(t-t')$. In this paper, we focus on the power-law form of the diffusion coefficient:

$$D(x) = \frac{D_0 l^\alpha}{|x|^\alpha}, \quad \text{with } \alpha > -1, \quad (6)$$

where D_0 is a positive constant that sets the strength of the noise and l is the length scale over which $D(x)$ changes. The exponent α quantifies the strength of the gradient of $D(x)$. Throughout this paper, we consider $\alpha > -1$ and choose the starting position at the origin (unless specified). Note that for $\alpha = 0$, $D(x) = D_0$ is just a constant and we recover the standard Brownian motion (SBm). However, our main interest, in this paper, lies in $\alpha \neq 0$ and compare it with the SBm.

Recall that the Langevin equation (5) does not uniquely specify the model for position-dependent diffusion coefficient and one also needs to specify the sense in which the stochastic integration of Eq. (5) is carried out [89, 90]. Throughout this paper, we will interpret Eq. (5) in Ito sense. Another problem that one encounters in simulation is $D(x)$ diverges as $|x| \rightarrow 0$ for $\alpha > 0$ while it tends to zero for $\alpha < 0$. Physically, this will cause the shooting off of particles to the infinity or accumulation around $x = 0$. In order to avoid this problem, we deploy the following form of $D(x)$ in simulation:

$$D(x) = \lim_{x_{\text{off}} \rightarrow 0^+} \frac{D_0 l^\alpha}{(|x| + x_{\text{off}})^\alpha}, \quad (\text{for simulation}). \quad (7)$$

On the other hand, for all our analytic calculations, we take the form of $D(x)$ in Eq. (6). Such x_{off} -considerations of $D(x)$ with power-law form have also been studied in [10–12]. For general α , the mean-squared displacement of $x(t)$ in Eq. (5) scales with time as $\langle x^2(t) \rangle \sim t^{\frac{2}{2+\alpha}}$ implying sub-diffusive behaviour for $\alpha > 0$, super-diffusive for $\alpha < 0$ and diffusive for $\alpha = 0$ [11]. Recently, this model was shown to display weak ergodicity breaking in the sense that time averaged and ensemble averaged MSDs are not identical [10].

Here, we look at the statistical properties of the maximum value $M(t)$ that the position $x(t)$ of the particle attains till duration t i.e., $M(t) = \max\{x(\tau)\}$, where $0 \leq \tau \leq t$ [see Figure 1]. In conjunction to this, we also investigate the statistics of the time $t_m(t)$ at which this maximum is reached. Exploiting the path-decomposition method for Markov processes [20], we derive exact expression for the joint distribution of $M(t)$ and $t_m(t)$ for all values of α . Marginalising this joint distribution provides the exact form of the distributions of $M(t)$ and $t_m(t)$.

Next, we also look at the statistics of residence time $t_r(t)$ which refers to the amount of time that the particle stays in $x > 0$ region till duration t . Formally, $t_r(t) = \int_0^t d\tau \Theta(x(\tau))$, where $\Theta(x)$ denotes the Heaviside theta function. Using the Feynman-Kac formalism [69, 91], we compute the exact probability distribution of $t_r(t)$ for all values of α . Finally, we study the last time $t_\ell(t)$ that the process $x(\tau)$ in Eq. (5) changes sign (or crosses the origin) till duration t and derive exact probability distribution for $t_\ell(t)$. An schematic illustration of M , t_m , t_r and t_ℓ for a typical trajectory of the particle is shown in Figure 1. Below, we summarise our main results:

1. For general α , we derive the exact probability distribution of the maximum M . Denoting this distribution by $P_m(M|t)$, we show that it possesses a scaling behaviour of the form

$$P_m(M|t) = \frac{1}{(\mathcal{D}_\alpha t)^{\frac{1}{2+\alpha}}} \mathcal{F}_\alpha \left(\frac{M}{(\mathcal{D}_\alpha t)^{\frac{1}{2+\alpha}}} \right), \quad (8)$$

where \mathcal{D}_α is a constant given in Eq. (27) and the scaling function $\mathcal{F}_\alpha(z)$ is defined as

$$\mathcal{F}_\alpha(z) = \frac{\mathcal{H}_{\frac{1}{2+\alpha}}(0)}{z^{\frac{3}{2+\alpha}}} \int_0^\infty dw e^{-\frac{w}{z^{2+\alpha}}} \mathbb{H}_{\frac{1}{2+\alpha}}(\sqrt{w}), \quad (9)$$

with $\mathcal{H}_{\frac{1}{2+\alpha}}(0) = \frac{2^{\frac{1}{2+\alpha}}}{\Gamma(\frac{1}{2+\alpha})}$ and the function $\mathbb{H}_\beta(w)$ given in Eq. (B9). For large z , we find that the scaling function decays as $\mathcal{F}_\alpha(z) \sim z^\alpha e^{-z^{2+\alpha}/4}$.

2. We next calculate the marginal probability distribution of the time $t_m(t)$ at which the maximum $M(t)$ is attained. We show that this distribution

possesses the scaling structure

$$\mathcal{P}_m(t_m|t) = \frac{1}{t} \mathcal{G}_m^\alpha \left(\frac{t_m}{t} \right), \quad (10)$$

with the scaling function $\mathcal{G}_m^\alpha(z)$ defined as

$$\mathcal{G}_m^\alpha(z) = \frac{(2+\alpha)\mathcal{H}_{\frac{1}{2+\alpha}}(0)}{2z^{\frac{1+\alpha}{2+\alpha}}(1-z)^{\frac{1}{2+\alpha}}} \int_0^\infty dw \frac{\mathbb{X}_\alpha \left(\sqrt{\frac{1-z}{zw^{2+\alpha}}} \right)}{\mathcal{H}_{\frac{1}{2+\alpha}} \left(w^{\frac{2+\alpha}{2}} \right)}. \quad (11)$$

The functions $\mathcal{H}_\beta(x)$ and $\mathbb{X}_\beta(x)$ are defined, respectively, in Eqs. (26) and (D7). Notice that the scaling function is not symmetric under the transformation $z \rightarrow 1-z$ for general α . Later, we show that it diverges as $\mathcal{G}_m^\alpha(z \rightarrow 0) \sim z^{-\frac{1+\alpha}{2+\alpha}}$ and $\mathcal{G}_m^\alpha(z \rightarrow 1) \sim (1-z)^{-\frac{1}{2}}$ at the two ends of z .

3. We also compute the distribution $\mathcal{P}_r(t_r|t)$ of the residence time t_r exactly. We show that it has the scaling form

$$\mathcal{P}_r(t_r|t) = \frac{1}{t} \mathcal{G}_r^\alpha \left(\frac{t_r}{t} \right), \quad (12)$$

with the scaling function $\mathcal{G}_r^\alpha(z)$ is given by

$$\begin{aligned} \mathcal{G}_r^\alpha(z) &= \frac{\sin \left(\frac{\pi}{2+\alpha} \right)}{\pi [z(1-z)]^{\frac{1+\alpha}{2+\alpha}}} \\ &\times \frac{1}{z^{\frac{2}{2+\alpha}} + (1-z)^{\frac{2}{2+\alpha}} + 2 \cos \left(\frac{\pi}{2+\alpha} \right) [z(1-z)]^{\frac{1}{2+\alpha}}}. \end{aligned} \quad (13)$$

This scaling function diverges as $\mathcal{G}_r^\alpha(z) \sim z^{-\frac{1+\alpha}{2+\alpha}}$ as $z \rightarrow 0$ and as $\mathcal{G}_r^\alpha(z) \sim (1-z)^{-\frac{1+\alpha}{2+\alpha}}$ as $z \rightarrow 1$.

4. Finally, we derive the probability distribution $\mathcal{P}_\ell(t_\ell|t)$ of the last-passage time t_ℓ which also possesses the scaling structure

$$\mathcal{P}_\ell(t_\ell|t) = \frac{1}{t} \mathcal{G}_\ell^\alpha \left(\frac{t_\ell}{t} \right), \quad (14)$$

with the scaling function $\mathcal{G}_\ell^\alpha(z)$ given by

$$\mathcal{G}_\ell^\alpha(z) = \frac{z^{-\frac{1+\alpha}{2+\alpha}} (1-z)^{-\frac{1}{2+\alpha}}}{\Gamma \left(\frac{1+\alpha}{2+\alpha} \right) \Gamma \left(\frac{1}{2+\alpha} \right)}. \quad (15)$$

Here, once again, we find that the scaling function does not retain symmetry under the transformation $z \rightarrow 1-z$ for $\alpha \neq 0$. Consequently, we get different behaviours of $\mathcal{G}_\ell^\alpha(z)$ for $z \rightarrow 0$ and $z \rightarrow 1$, viz. $\mathcal{G}_\ell^\alpha(z \rightarrow 0) \sim z^{-\frac{1+\alpha}{2+\alpha}}$ and $\mathcal{G}_\ell^\alpha(z \rightarrow 1) \sim (1-z)^{-\frac{1}{2+\alpha}}$.

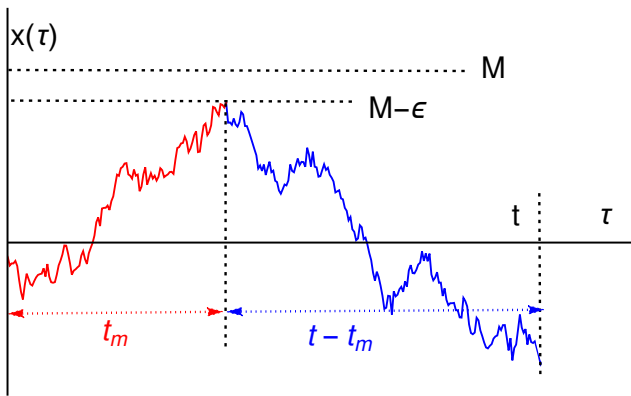


FIG. 2. Schematic of a typical trajectory of the particle in which it reaches $M-\epsilon$ at time t_m for the first time and remains below M in the remaining time $t-t_m$. The trajectory can be decomposed into two parts: from 0 to t_m (shown in red) and from t_m to t (shown in blue).

We remark that all the scaling functions written above converge to that of the SBm for $\alpha = 0$. Recall that the distributions of t_m , t_r and t_ℓ are all identical for $\alpha = 0$, *à la* “arcsine laws” due to Lévy [19]. However, our study reveals that they are significantly different for $\alpha \neq 0$. Also, contrary to the SBm, we saw above that the distributions of t_m and t_ℓ for $\alpha \neq 0$ have asymmetric peaks (divergences) as $t_i \rightarrow 0^+$ and $t_i \rightarrow t^-$ where $t_i \in \{t_m, t_\ell\}$. All these observations exemplify that the properties of M , t_m , t_r and t_ℓ for $\alpha \neq 0$ are remarkably different than that of the SBm. In the following, we provide a detailed analysis of these quantities and point out the key differences for $\alpha \neq 0$.

III. EXTREME VALUE M AND TIME t_m TO REACH MAXIMUM

We first consider the joint distribution $\mathcal{P}(M, t_m|t)$ of the maximum displacement M and the time t_m at which the maximum is attained till duration t . The initial position is fixed to the origin. To compute this distribution, we decompose the trajectory in two parts: (i) the part from 0 to t_m and (ii) the part from t_m to t . They are shown schematically in Figure 2 where the red half corresponds to the first part and the blue half represents the second part. Since the process is Markovian, the two parts are statistically independent.

Let us now calculate the contribution of each part. In part (i), the time t_m is just the first-passage time to $x = M$ starting from the origin. Therefore, the probability weight in this part is just the first-passage time distribution $F_M(t_m|0)$ to reach M for the first time at t_m given that the particle was initially at $x = 0$. For part (ii), the process remains below $x = M$ in the interval $t-t_m$ such that the particle was at $x = M$ at time t_m . Hence, the weight of this part is given by the survival probability $S_M(t-t_m|M)$ where we have used

the notation $S_{x_m}(\tau|x_0)$ to denote the probability that the particle has not crossed $x = x_m$ up to time τ starting from $x = x_0$. Note that the process remains below $x = M$ in both parts. However, as shown later, it turns out that $S_M(\tau|M) = 0$ for all non-zero τ . To circumvent this problem, we follow the procedure in [20, 28] where we compute $F_{M-\epsilon}(t_m|0)$ and $S_M(t-t_m|M-\epsilon)$ instead of $F_M(t_m|0)$ and $S_M(t-t_m|M)$ and later take the $\epsilon \rightarrow 0^+$ limit. The joint distribution $\mathcal{P}(M, t_m|t)$ can then be written as

$$\mathcal{P}(M, t_m|t) = \frac{F_{M-\epsilon}(t_m|0) S_M(t-t_m|M-\epsilon)}{\mathcal{N}(\epsilon)}. \quad (16)$$

Here $1/\mathcal{N}(\epsilon)$ is the proportionality constant independent of t and t_m . It turns out convenient to take double Laplace transformation of Eq. (16) with respect to t_m ($\rightarrow p$) and t ($\rightarrow s$). For a general function $g(t)$, the Laplace transformation with respect to t is defined as

$$\bar{g}(s) = \int_0^\infty dt e^{-st} g(t), \quad (17)$$

and the inverse Laplace transformation is defined in terms of the Bromwich integral as

$$g(t) = \mathcal{L}_{s \rightarrow t}[\bar{g}(s)] = \frac{1}{2\pi i} \int_{\gamma+i\infty}^{\gamma-i\infty} ds e^{st} \bar{g}(s), \quad (18)$$

where γ is the vertical contour in the complex s -plane such that all singularities of $\bar{g}(s)$ lie to its left.

Taking the double Laplace transformation of Eq. (16) gives

$$\bar{P}(M, p|s) = \frac{\bar{F}_{M-\epsilon}(s+p|0) \bar{S}_M(s|M-\epsilon)}{\mathcal{N}(\epsilon)}, \quad (19)$$

where $\bar{P}(M, p|s)$ is the double Laplace transformation of $\mathcal{P}(M, t_m|t)$. Quite remarkably, the joint distribution of M and t_m has now been completely specified in terms of the survival probability and first-passage time distribution. In what follows, we use the standard techniques to calculate these distributions and probabilities and then use Eq. (19) to compute the joint distribution.

A. Survival probability $S_M(t|x_0)$

Let us focus on the survival probability $S_M(t|x_0)$ for our model in Eq. (5). For simplicity, we consider $M \geq 0$ and $x_0 \leq M$ which is also consistent with our main aim of computing the joint distribution in Eq. (19). In Ito setup, $S_M(t|x_0)$ obeys the backward Fokker Planck equation [92]

$$\partial_t S_M(t|x_0) = D(x_0) \partial_{x_0}^2 S_M(t|x_0), w \quad (20)$$

with $D(x_0)$ defined in Eq. (6). Our aim is to solve this equation for general α . In order to solve it, we have to specify the appropriate initial condition and boundary

conditions. Initially, the particle starts from the position x_0 which is different from the position of the absorbing wall at $x = M$. Consequently, we have

$$S_M(0|x_0) = 1. \quad (21)$$

Next, we specify the boundary conditions which read

$$S_M(t|x_0 \rightarrow M^-) = 0, \quad (22)$$

$$S_M(t|x_0 \rightarrow -\infty) = 1. \quad (23)$$

To understand the boundary condition in Eq. (22), note that if the particle initially starts from $x_0 \rightarrow M^-$, then it will immediately get absorbed. This results in the zero survival probability. On the other hand, if the particle is at $x_0 \rightarrow -\infty$, then it will survive the barrier at $x = M$ for all finite time. This gives rise to the second boundary condition in Eq. (23).

To solve Eq. (20), we take Laplace transformation with respect to t ($\rightarrow s$) and rewrite

$$s\bar{S}_M(s|x_0) - 1 = D(x_0)\partial_{x_0}^2\bar{S}_M(s|x_0). \quad (24)$$

The boundary conditions can also be suitably translated in terms of $\bar{S}_M(s|x_0)$. Fortunately, one can solve Eq. (24) for general α . To maintain the continuity of presentation, we have presented the details of the solution in appendix A and present only the final result here. For $x_0 \geq 0$, we find

$$\bar{S}_M(s|x_0) = \frac{1}{s} \left[1 - \frac{\mathcal{H}_{\frac{1}{2+\alpha}}\left((a_s x_0)^{\frac{2+\alpha}{2}}\right)}{\mathcal{H}_{\frac{1}{2+\alpha}}\left((a_s M)^{\frac{2+\alpha}{2}}\right)} \right], \quad (25)$$

where the function $\mathcal{H}_\beta(x_0)$ is defined as

$$\mathcal{H}_\beta(x_0) = x_0^\beta [I_\beta(x_0) + I_{-\beta}(x_0)], \quad (26)$$

$$a_s = \left(\frac{s}{D_\alpha}\right)^{\frac{1}{2+\alpha}}, \quad \text{with } D_\alpha = \frac{D_0 l^\alpha (2+\alpha)^2}{4}. \quad (27)$$

Here, $I_\beta(x_0)$ is the modified Bessel function of first kind. Below, we use $\bar{S}_M(s|x_0)$ from Eq. (25) to calculate the joint distribution $\bar{P}(M, p|s)$ in Eq. (19).

B. Joint probability distribution $\mathcal{P}(M, t_m|t)$

Looking at the expression of $\bar{P}(M, p|s)$ in Eq. (19), we need to specify the Laplace transformations $\bar{S}_M(s|M-\epsilon)$ and $\bar{F}_{M-\epsilon}(s+p|0)$ in the limit $\epsilon \rightarrow 0^+$. Using Eq. (25), these Laplace transforms can be easily calculated up to leading order in ϵ as

$$\bar{S}_M(s|M-\epsilon) \simeq \frac{\epsilon \partial_M \left[\mathcal{H}_{\frac{1}{2+\alpha}}\left((a_s M)^{\frac{2+\alpha}{2}}\right) \right]}{s \mathcal{H}_{\frac{1}{2+\alpha}}\left((a_s M)^{\frac{2+\alpha}{2}}\right)}, \quad (28)$$

$$\begin{aligned} \bar{F}_{M-\epsilon}(s+p|0) &= 1 - (s+p) \bar{S}_{M-\epsilon}(s+p|0), \\ &\simeq \frac{\mathcal{H}_{\frac{1}{2+\alpha}}(0)}{\mathcal{H}_{\frac{1}{2+\alpha}}\left((a_{s+p} M)^{\frac{2+\alpha}{2}}\right)}. \end{aligned} \quad (29)$$

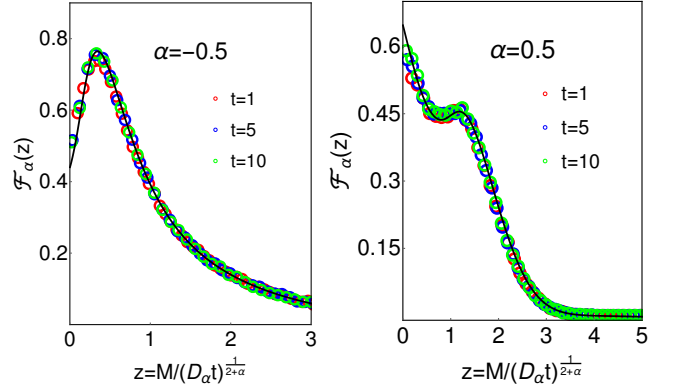


FIG. 3. Scaling function $\mathcal{F}_\alpha(z)$ in Eq. (9) is plotted for two values of α . In both panels, solid black line represents the analytic expression in Eq. (9) and the circles represent simulation data. We have chosen $D_0 = 0.1$ and $l = 1$

Inserting these expressions in Eq. (19) gives $\bar{P}(M, p|s)$ as

$$\begin{aligned} \bar{P}(M, p|s) &= \frac{\epsilon \mathcal{H}_{\frac{1}{2+\alpha}}(0)}{\mathcal{N}(\epsilon) s \mathcal{H}_{\frac{1}{2+\alpha}}\left((a_{s+p} M)^{\frac{2+\alpha}{2}}\right)} \\ &\quad \times \frac{\partial_M \left[\mathcal{H}_{\frac{1}{2+\alpha}}\left((a_s M)^{\frac{2+\alpha}{2}}\right) \right]}{\mathcal{H}_{\frac{1}{2+\alpha}}\left((a_s M)^{\frac{2+\alpha}{2}}\right)}. \end{aligned} \quad (30)$$

The task now is to evaluate the function $\mathcal{N}(\epsilon)$. For this, we use the normalisation condition of $\mathcal{P}(M, t_m|t)$ which in terms of the Laplace transform $\bar{P}(M, p|s)$ becomes

$$\int_0^\infty dM \bar{P}(M, p=0|s) = \frac{1}{s}. \quad (31)$$

It is now easy to show that $\mathcal{N}(\epsilon) = \epsilon$. Substituting this in Eq. (30) yields

$$\begin{aligned} \bar{P}(M, p|s) &= \frac{\mathcal{H}_{\frac{1}{2+\alpha}}(0)}{s \mathcal{H}_{\frac{1}{2+\alpha}}\left((a_{s+p} M)^{\frac{2+\alpha}{2}}\right)} \\ &\quad \times \frac{\partial_M \left[\mathcal{H}_{\frac{1}{2+\alpha}}\left((a_s M)^{\frac{2+\alpha}{2}}\right) \right]}{\mathcal{H}_{\frac{1}{2+\alpha}}\left((a_s M)^{\frac{2+\alpha}{2}}\right)}. \end{aligned} \quad (32)$$

To summarise, we have exactly computed the joint distribution of $M(t)$ and $t_m(t)$ in terms of the Laplace variables p and s . To get distribution in the time domain, one has to perform double inverse Laplace transformations which, unfortunately, turns out to be challenging. However, one could still obtain the explicit expressions of the marginal distributions of $M(t)$ and $t_m(t)$ by appropriately integrating $\bar{P}(M, p|s)$. In what follows, we look at the marginal distribution of the maximum $M(t)$ followed by that of the arg-max $t_m(t)$.

C. Marginal distribution $P_m(M|t)$ of $M(t)$

To get the marginal distribution $P_m(M|t)$ of the maximum M , we need to integrate the joint distribution $\mathcal{P}(M, t_m|t)$ over all t_m . This is equivalent to putting $p = 0$ in the expression of $\bar{P}(M, p|s)$ in Eq. (32). The Laplace transform of $P_m(M|t)$ then reads

$$\begin{aligned} \bar{P}_m(M|s) &= \bar{P}(M, p = 0|s), \\ &= -\frac{d\bar{J}(M, s)}{dM}, \quad \text{with} \end{aligned} \quad (33)$$

$$\bar{J}(M, s) = \frac{\mathcal{H}_{\frac{1}{2+\alpha}}(0)}{s \mathcal{H}_{\frac{1}{2+\alpha}}\left((a_s M)^{\frac{2+\alpha}{2}}\right)}. \quad (34)$$

The task is now to perform the inverse Laplace transformation. Fortunately, the inversion can be exactly carried out by using the Bromwich integral in Eq. (18). We provide the details of this calculation in appendix B. The distribution $P_m(t_m|t)$ possesses the scaling form in $M/t^{\frac{1}{2+\alpha}}$ as written in (8) with the scaling function $\mathcal{F}_\alpha(z)$ defined in (9).

Few remarks are in order. Firstly, for $\alpha = 0$ (homogeneous case), we find $\mathbb{H}_{\frac{1}{2}}(w)$ in Eq. (B9) has the simple form

$$\mathbb{H}_{\frac{1}{2}}(w) = \sqrt{\frac{2}{\pi}} \sin(w). \quad (35)$$

Inserting this in the expression of the scaling function $\mathcal{F}_\alpha(z)$ in (9) and performing the integration over w yields

$$\mathcal{F}_\alpha(z) = \frac{e^{-z^2/4}}{\sqrt{\pi}}, \quad (\text{for } \alpha = 0). \quad (36)$$

This matches with the distribution of M for the standard Brownian motion in Eq. (1). We remark that the scaling of the maximum with time as $M \sim t^{\frac{1}{2+\alpha}}$ is quite expected since the position also scales as $x \sim t^{\frac{1}{2+\alpha}}$. However, our analysis goes beyond this scaling behaviour and also provides exact form of the scaling function for all values of α .

In Figure 3, we have plotted $\mathcal{F}_\alpha(z)$ and compared it against the simulation for two different values of α . For each value, we have considered three different values of t . We see excellent match of our analytic results with the simulations. To contrast these results with that of the standard Brownian motion, we look at the asymptotic behaviour of $\mathcal{F}_\alpha(z)$ for different z . In particular, for $\alpha \neq 0$, we have shown in appendix C that the scaling function has the following asymptotic forms:

$$\mathcal{F}_\alpha(z) \simeq \frac{1}{C_\alpha \Gamma\left(\frac{1+\alpha}{2+\alpha}\right)} - \frac{2z}{C_\alpha^2 \Gamma\left(\frac{\alpha}{2+\alpha}\right)}, \quad \text{as } z \rightarrow 0, \quad (37)$$

$$\simeq \frac{(2+\alpha)\mathcal{H}_{\frac{1}{2+\alpha}}(0)}{2^{\frac{3+2\alpha}{2+\alpha}}} z^\alpha e^{-\frac{z^{2+\alpha}}{4}}, \quad \text{as } z \rightarrow \infty, \quad (38)$$

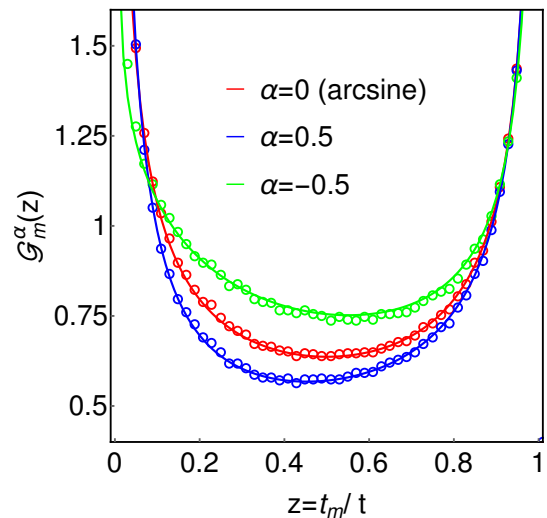


FIG. 4. We have plotted the scaling function $\mathcal{G}_m^\alpha(z)$ of arg-maximum t_m in Eq. (11) for three different values of α . The circles represent the comparison of numerical simulations with the analytic expression (shown by solid line). Parameters chosen are $D_0 = 0.1$, $l = 1$ and $t = 5$.

where $C_\alpha = \frac{2^{2/2+\alpha} \Gamma\left(\frac{1}{2+\alpha}\right)}{(2+\alpha) \Gamma\left(\frac{1+\alpha}{2+\alpha}\right)}$. On the other hand for $\alpha = 0$, one as

$$\mathcal{F}_0(z) \simeq \frac{1}{\sqrt{\pi}} \left(1 - \frac{z^2}{4}\right), \quad \text{as } z \rightarrow 0, \quad (39)$$

$$= \frac{e^{-z^2/4}}{\sqrt{\pi}}, \quad \text{as } z \rightarrow \infty. \quad (40)$$

We see that while, for $\alpha = 0$, the scaling function decreases quadratically with z as $z \rightarrow 0$, it changes linearly for $\alpha \neq 0$ [see Eq. (37)]. Also, the small z behaviour is rather different for $\alpha < 0$ and $\alpha > 0$. For $\alpha < 0$, we see, in Figure 3 (left panel), that $\mathcal{F}_\alpha(z)$ rises initially with z , attains a maximum value and then decreases again for z . On the other hand, for $\alpha > 0$, we see that $\mathcal{F}_\alpha(z)$ initially decreases with z , then rises at some intermediate z until it attains a local maximum. After that, it again decreases for large z (see Figure 3 (right panel)). Interestingly, in contrast to the standard Brownian motion ($\alpha = 0$), we see that $\mathcal{F}_\alpha(z)$ show non-monotonic dependence on z for all $\alpha \neq 0$ (see Figure 3).

D. Marginal distribution $\mathcal{P}_m(t_m|t)$ of $t_m(t)$

We now analyse the Laplace transform $\bar{P}(M, p|s)$ of the joint distribution in Eq. (32) to calculate the probability distribution $\mathcal{P}_m(t_m|t)$ of the arg-maximum $t_m(t)$.

Integrating $\bar{P}(M, p|s)$ with respect to M gives

$$\bar{\mathcal{P}}_m(p|s) = \int_0^\infty dM \frac{\mathcal{H}_{\frac{1}{2+\alpha}}(0)}{s \mathcal{H}_{\frac{1}{2+\alpha}}\left(\left(a_{s+p}M\right)^{\frac{2+\alpha}{2}}\right)} \times \frac{\partial_M \left[\mathcal{H}_{\frac{1}{2+\alpha}}\left(\left(a_s M\right)^{\frac{2+\alpha}{2}}\right) \right]}{\mathcal{H}_{\frac{1}{2+\alpha}}\left(\left(a_s M\right)^{\frac{2+\alpha}{2}}\right)}, \quad (41)$$

where $\bar{\mathcal{P}}_m(p|s)$ is just the double Laplace transformation of $\mathcal{P}_m(t_m|t)$ with respect to t_m ($\rightarrow p$) and t ($\rightarrow s$). To simplify this equation further, we use

$$\frac{d}{dy} \mathcal{H}_{\frac{1}{2+\alpha}}\left(y^{\frac{2+\alpha}{2}}\right) = \left(\frac{2+\alpha}{2}\right) \mathcal{H}_{\frac{1+\alpha}{2+\alpha}}\left(y^{\frac{2+\alpha}{2}}\right)$$

and change the variable $a_{s+p}M = w$. Eq. (41) can then be rewritten as

$$\bar{\mathcal{P}}_m(p|s) = \frac{\mathcal{H}_{\frac{1}{2+\alpha}}(0)}{2(2+\alpha)^{-1}} \int_0^\infty dw \frac{\bar{\mathbb{Y}}_\alpha(s, p, w)}{\mathcal{H}_{\frac{1}{2+\alpha}}\left(w^{\frac{2+\alpha}{2}}\right)}, \quad \text{with} \quad (42)$$

$$\bar{\mathbb{Y}}_\alpha(s, p, w) = \frac{1}{s^{\frac{1+\alpha}{2+\alpha}}(s+p)^{\frac{1}{2+\alpha}}} \frac{\mathcal{H}_{\frac{1+\alpha}{2+\alpha}}\left(w^{\frac{2+\alpha}{2}}\right)}{\mathcal{H}_{\frac{1}{2+\alpha}}\left(w^{\frac{2+\alpha}{2}}\right)}. \quad (43)$$

To get the distribution in time domain, one needs to perform the double inverse Laplace transformation of $\bar{\mathbb{Y}}_\alpha(s, p, w)$. In appendix D, we have explicitly carried out this inversion. The final forms of the distribution show that $\mathcal{P}_m(t_m|t)$ possesses the scaling form as quoted in Eq.(10) where the scaling function $\mathcal{G}_m^\alpha(z)$ is given in Eq. (11).

In Figure 4, we have illustrate this scaling behaviour for different values of α . For all values, we see excellent agreement of our analytic results with the numerical simulations. For $\alpha = 0$, using $\mathbb{X}_0(x) = \pi^{-1}$ from Eq. (D7) and $\mathcal{H}_{\frac{1}{2}}(x) = \sqrt{\frac{2}{\pi}} e^x$ from Eq. (26), it is straightforward to show that the scaling function in Eq. (11) becomes

$$\mathcal{G}_m^\alpha(z) = \frac{1}{\pi \sqrt{z(1-z)}}, \quad (\text{for } \alpha = 0)$$

which matches with the *arcsine law* in Eq. (2). Curiously, the scaling function $\mathcal{G}_m^\alpha(z)$ is symmetric under the transformation $z \rightarrow 1-z$ only for $\alpha = 0$. On the other hand, for non-zero α , we see that $\mathcal{G}_m^\alpha(z)$ is not symmetric under this transformation. To see this clearly, let us look at the form of $\mathcal{G}_m^\alpha(z)$ for $z \rightarrow 0$ and $z \rightarrow 1$. For general α , we find (see appendix E) that the scaling function diverges as $\mathcal{G}_m^\alpha(z \rightarrow 0) \sim z^{-\frac{1+\alpha}{2+\alpha}}$ and $\mathcal{G}_m^\alpha(z \rightarrow 1) \sim (1-z)^{-\frac{1}{2}}$. Clearly, the divergences at two ends are asymmetric for all $\alpha \neq 0$. Surprisingly, the divergence of the scaling function as $z \rightarrow 1$ is completely universal characterised by an α -independent exponent $1/2$. The prefactor, however, may depend on

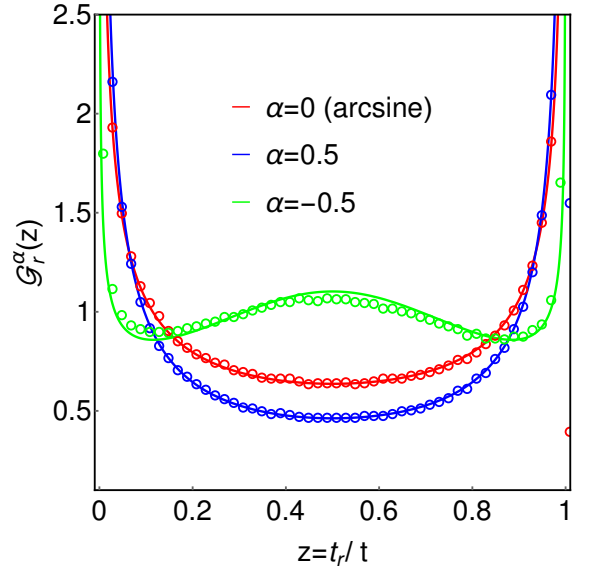


FIG. 5. Scaling function $\mathcal{G}_r^\alpha(z)$ in Eq. (13) for the occupation time distribution is plotted and compared with the numerical simulation for three different values of α . The analytic expression in Eq. (13) is shown in solid line and the simulation data are shown by circles. We have chosen $D_0 = 0.1$, $l = 1$ and $t = 5$.

the value of α as illustrated in appendix E. Heuristically, this α -independence divergence can be understood as follows: From Eq. (16), we see that the joint distribution $\mathcal{P}(M, t_m|t)$ is proportional to the survival probability $S_M(t - t_m|M - \epsilon)$ which for $t_m \rightarrow t^-$ scales as $S_M(t - t_m|M - \epsilon) \sim (t - t_m)^{-1/2}$ for all values of α [see Eq. (28)]. Consequently, the marginal distribution $\mathcal{P}_m(t_m|t)$ diverges as $(t - t_m)^{-1/2}$.

IV. RESIDENCE TIME DISTRIBUTION $\mathcal{P}_r(t_r|t)$

Residence time refers to the amount of time that particle spends in the $x > 0$ region till duration t . It is defined as $t_r(t) = \int_0^t d\tau \Theta(x(\tau))$, where $\Theta(x)$ denotes the Heaviside theta function. The distribution of $t_r(t)$ has been studied for a variety of stochastic processes [see discussion below Eq. (4)]. For standard Brownian motion, the distribution of $t_r(t)$ is given in Eq. (3). As evident that this distribution diverges at $t_r = 0$ and $t_r = t$, whereas it exhibits minimum value at $t_r = t/2$. This implies rather a counter-intuitive property of the Brownian motion where once it crosses the origin on positive or negative side, it is reluctant to come back [69]. A natural question is: what happens to this property for general α ? In order to answer this question, we look at the residence time distribution for general α in this section.

Let us denote the distribution of t_r by $\mathcal{P}_r(t_r, x_0|t)$ where x_0 is the initial position and t is the total observation time. We represent the Laplace transformation of

$\mathcal{P}_r(t_r, x_0|t)$ with respect to t_r as $\mathcal{Q}(p, x_0|t)$.

$$\mathcal{Q}(p, x_0|t) = \langle e^{-pt_r} \rangle, \quad (44)$$

$$= \int_0^\infty dt_r e^{-pt_r} \mathcal{P}_r(t_r, x_0|t). \quad (45)$$

The Laplace transform $\mathcal{Q}(p, x_0|t)$ satisfies the following backward master equations [69]:

$$\partial_t \mathcal{Q}(p, x_0|t) = [D(x_0) \partial_{x_0}^2 - p \Theta(x_0)] \mathcal{Q}(p, x_0|t), \quad (46)$$

where $D(x_0)$ is defined in Eq. (6). In order to solve this equation, we also need to specify the initial and boundary conditions. For initial condition, we note that if $t \rightarrow 0$, then the residence time t_r also tends to zero, i.e. $t_r \rightarrow 0$. Using this in Eq. (44), we obtain

$$\mathcal{Q}(p, x_0|t \rightarrow 0) = 1. \quad (47)$$

On the other hand, for any finite t , we have the following boundary conditions:

$$\mathcal{Q}(p, x_0 \rightarrow -\infty|t) = 1, \quad (48)$$

$$\mathcal{Q}(p, x_0 \rightarrow \infty|t) = e^{-pt}. \quad (49)$$

Note that the first boundary condition follows from the fact that if $x_0 \rightarrow -\infty$, then the particle essentially stays in the $x < 0$ region for all finite t . Consequently $t_r = 0$ which from Eq. (44) leads to $\mathcal{Q}(p, x_0 \rightarrow -\infty|t) = 1$. On the other hand, if $x_0 \rightarrow \infty$, then the particle stays in $x > 0$ region for all finite t and $t_r = t$. This results in the second boundary condition in Eq. (49).

We now proceed to solve the backward equation (46) with these initial and boundary conditions. To this aim, we take another Laplace transformation of $\mathcal{Q}(p, x_0|t)$ with respect to t and denote it by $\bar{\mathcal{Q}}(p, x_0|s)$. One can then appropriately transform the backward equation in terms of $\bar{\mathcal{Q}}(p, x_0|s)$ and solve it. To maintain continuity of the presentation, we have relegated these details appendix F and write only the final solution here. For $x_0 = 0$, we find

$$\bar{\mathcal{Q}}(p|s) = \frac{1}{s} - \frac{p}{s(s+p)} \left[1 + \left(\frac{s}{s+p} \right)^{\frac{1}{2+\alpha}} \right]^{-1}, \quad (50)$$

where we have used the short hand notation $\bar{\mathcal{Q}}(p|s) = \bar{\mathcal{Q}}(p, x_0 = 0|s)$. Fortunately, this Laplace transform can be exactly inverted for all α [78, 86]. The distribution $\mathcal{P}_r(t_r|t)$ indeed has the scaling form in Eq. (12) and the scaling function $\mathcal{G}_r^\alpha(z)$ is given in Eq. (13).

For $\alpha = 0$, we recover the *arcsine law* in Eq. (3). In Figure 5, we have illustrated the scaling function $\mathcal{G}_r^\alpha(z)$ for three different values of α and compared them against the simulation. We find excellent agreement between them. Contrary to the arg-maximum $t_m(t)$, we see that the $\mathcal{G}_r^\alpha(z)$ is symmetric about $z = \frac{1}{2}$ and diverges as $z^{-\frac{1+\alpha}{2+\alpha}}$ and $(1-z)^{-\frac{1+\alpha}{2+\alpha}}$ as $z \rightarrow 0$ and $z \rightarrow 1$ respectively. Interestingly, in Figure 5, we see that the scaling function

exhibits local maxima at $z = 1/2$ for $\alpha = -0.5$ which is in contrast to the other two values of α for which one finds minima at $z = 1/2$. To understand this behaviour, we analyse $\mathcal{G}_r^\alpha(z)$ in the vicinity of $z = 1/2$. Expanding $\mathcal{G}_r^\alpha(z)$ in Eq. (13) for $z = \frac{1+\bar{\epsilon}}{2}$ with $\bar{\epsilon} \rightarrow 0$, we get

$$\mathcal{G}_r^\alpha \left(\frac{1+\bar{\epsilon}}{2} \right) \simeq \frac{2}{\pi} \tan \left(\frac{\pi}{2(2+\alpha)} \right) + \frac{\mathbb{K}(\alpha) \bar{\epsilon}^2}{2\pi}, \quad (51)$$

where the function $\mathbb{K}(\alpha)$ is defined as

$$\mathbb{K}(\alpha) = \frac{\left[2 + \alpha(4 + \alpha) + (2 + \alpha)^2 \cos \left(\frac{\pi}{2+\alpha} \right) \right]}{(2 + \alpha)^2 \sin^{-1} \left(\frac{\pi}{2+\alpha} \right) \sec^{-4} \left(\frac{\pi}{2(2+\alpha)} \right)}. \quad (52)$$

Now, $\mathcal{G}_r^\alpha(z)$ will exhibit local maxima or minima at $z = 1/2$ depending on whether $\mathbb{K}(\alpha)$ is positive or negative. Defining the critical value of α as

$$\mathbb{K}(\alpha_c) = 0, \implies \alpha_c \simeq -0.3182, \quad (53)$$

we find that $\mathbb{K}(\alpha) > 0$ for $\alpha \geq \alpha_c$ and $\mathbb{K}(\alpha) < 0$ for $\alpha < \alpha_c$. Therefore, we expect a local maxima at $z = 1/2$ for the scaling function $\mathcal{G}_r^\alpha(z)$ for $\alpha < \alpha_c$. Quite remarkably, this implies that for $\alpha \geq \alpha_c$, the particle typically tends to stay on one side of the origin which is reminiscent of the standard Brownian motion. On the other hand, for $\alpha < \alpha_c$, the probability to cross the origin increases which results in the local maxima of $\mathcal{G}_r^\alpha(z)$ at $z = 1/2$. In fact, as $\alpha \rightarrow -1$, the scaling function simply becomes $\delta(z - 1/2)$. This implies that the particle spends equal amount of time on the positive and negative sides of the origin which is in sharp contrast to the standard Brownian motion.

V. LAST PASSAGE TIME DISTRIBUTION

$$\mathcal{P}_\ell(t_\ell|t)$$

We now study the probability distribution $\mathcal{P}_\ell(t_\ell|t)$ of time t_ℓ that the particle crosses origin for the last time till duration t . As illustrated in Figure 1, we can analyse this problem by decomposing the trajectory into two parts. In the first part, particle reaches the origin at time t_ℓ after starting its motion initially from the origin. The weight of this part is just the free probability distribution $\mathbb{P}(0, t_\ell|0)$. In the second part, particle does not cross the origin in the remaining time interval $(t - t_\ell)$ given that it was at the origin at time t_ℓ . Then, the contribution of this part to $\mathcal{P}_\ell(t_\ell|t)$ is the survival probability $S_0(t - t_\ell|0)$. Since the process is Markovian, these two contributions are statistically independent.

However, one encounters similar problem as encountered for the case of extreme value statistics in sec. III. Recall from this analysis of extreme value statistics that $S_0(t - t_\ell|0)$ is exactly equal to zero for all $t - t_\ell$. In order to circumvent this problem, we instead compute the quantities $\mathbb{P}(\epsilon, t_\ell|0)$ and $S_0(t - t_\ell|\epsilon)$ and take $\epsilon \rightarrow 0^+$

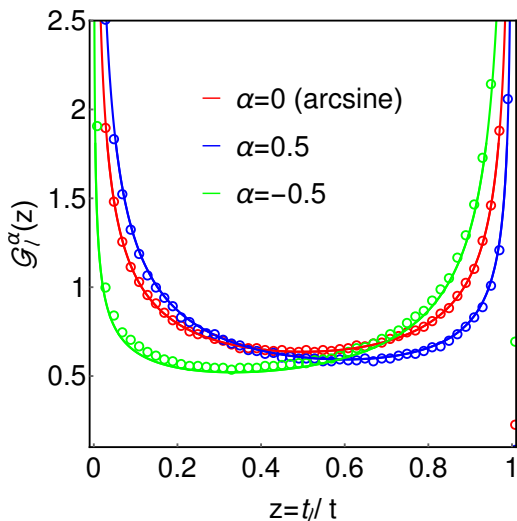


FIG. 6. Scaling function $\mathcal{G}_\ell^\alpha(z)$ in Eq. (15) for the last passage time distribution is plotted and compared with the numerical simulation for three different values of α . The analytic expression in Eq. (15) is shown in solid line and the simulation data are shown by circles. We have chosen $D_0 = 0.1$, $l = 1$ and $t = 5$.

limit at an appropriate stage of the calculation. Then, the distribution $\mathcal{P}_\ell(t_\ell|t)$ can be written as

$$\mathcal{P}_\ell(t_\ell|t) = \frac{\mathbb{P}(\epsilon, t_\ell|0) S_0(t - t_\ell|\epsilon)}{\mathcal{N}_L(\epsilon)}, \quad (54)$$

where the function $\mathcal{N}_L(\epsilon)$ is the normalisation factor. It is instructive to take the double Laplace transformation of this equation with respect to t_ℓ ($\rightarrow p$) and t ($\rightarrow s$) to get

$$\bar{\mathcal{P}}_\ell(p|s) = \frac{\bar{\mathbb{P}}(\epsilon, s + p|0) \bar{S}_0(s|\epsilon)}{\mathcal{N}_L(\epsilon)}. \quad (55)$$

Hence, the task now is to calculate the Laplace transforms of the survival probability and distribution in an infinite line. In appendix G, we have calculated these Laplace transforms explicitly for $\epsilon \rightarrow 0$ limit. Here, we present only the final expressions:

$$\bar{\mathbb{P}}(\epsilon, s|0) \simeq \frac{\mathcal{A}_L(\epsilon)}{s^{\frac{1}{2+\alpha}}}, \quad (56)$$

$$\bar{S}_0(s|\epsilon) \simeq \frac{\mathcal{B}_L(\epsilon)}{s^{\frac{1+\alpha}{2+\alpha}}}, \quad (57)$$

where $\mathcal{A}_L(\epsilon)$ and $\mathcal{B}_L(\epsilon)$ are functions of ϵ whose explicit forms are given in Eqs. (G12) and (G14) respectively. Next, we insert Eqs. (56) and (57) in Eq. (55) to write $\bar{\mathcal{P}}_\ell(p|s)$ as

$$\bar{\mathcal{P}}_\ell(p|s) \simeq \frac{\mathcal{A}_L(\epsilon) \mathcal{B}_L(\epsilon)}{\mathcal{N}_L(\epsilon)} \frac{1}{s^{\frac{1+\alpha}{2+\alpha}} (s+p)^{\frac{1}{2+\alpha}}}. \quad (58)$$

We now have to specify the normalisation factor $\mathcal{N}_L(\epsilon)$. To evaluate this factor, we use the normalisation condition $\bar{\mathcal{P}}_\ell(0|s) = 1/s$ from which it is easy to show that $\mathcal{N}_L(\epsilon) = \mathcal{A}_L(\epsilon) \mathcal{B}_L(\epsilon)$. This leads us to write $\bar{\mathcal{P}}_\ell(p|s)$ as

$$\bar{\mathcal{P}}_\ell(p|s) = \frac{1}{s^{\frac{1+\alpha}{2+\alpha}} (s+p)^{\frac{1}{2+\alpha}}}. \quad (59)$$

Finally, performing the double inverse Laplace transformation of this equation, we find that the distribution $\mathcal{P}_\ell(t_\ell|t)$ of the last passage time t_ℓ indeed possesses the scaling behaviour of Eq. (14) with the scaling function $\mathcal{G}_\ell^\alpha(z)$ defined in Eq. (15) for general α . In Figure 6, we have plotted $\mathcal{G}_\ell^\alpha(z)$ for three values of α and compared against the numerical simulations. We observe excellent match for all α .

It is worth remarking that $\mathcal{G}_\ell^\alpha(z)$ possesses $z \rightarrow 1 - z$ symmetry only for $\alpha = 0$. However, the symmetry is absent for non-zero values for α as elucidated in Figure 6. Consequently, we get different divergences of the scaling function at the two ends, i.e. $\mathcal{G}_\ell^\alpha(z \rightarrow 0) \sim z^{-\frac{1+\alpha}{2+\alpha}}$ and $\mathcal{G}_\ell^\alpha(z \rightarrow 1) \sim (1-z)^{-\frac{1}{2+\alpha}}$. Physically, this asymmetric nature can be understood in the following way: For $\alpha > 0$, the particle typically stays away from the origin due to the large values of the diffusion coefficient around the origin. This gives rise to the smaller values of t_ℓ . As a result, the distribution $\mathcal{P}_\ell(t_\ell|t)$ is sharply peaked at the smaller values of t_ℓ . On the other hand, for $\alpha < 0$, the particle typically stays near the origin which enhances its chances to cross the origin. This essentially gives rise to the large values of t_ℓ and peaking of $\mathcal{P}_\ell(t_\ell|t)$ at these values.

VI. CONCLUSION

To conclude, we have studied a model of anomalous diffusion in which a single particle moves in an one dimensional heterogeneous medium with spatially varying diffusion coefficient of the form $D(x) \sim |x|^{-\alpha}$ with $\alpha > -1$. Depending on the exponent α , this model displays super-diffusive ($-1 < \alpha < 0$), diffusive ($\alpha = 0$) or sub-diffusive ($0 < \alpha < \infty$) scaling of the mean-squared displacement (MSD). Curiously, this simple Markov process also exhibits weak ergodicity breaking in the sense that the time-averaged and ensemble averaged MSDs are not equal even at large times [10–16].

In this paper, we extensively investigated the statistical properties of the maximum displacement $M(t)$ and time $t_m(t)$ taken to reach this maximum till duration t . Exploiting the path decomposition technique for Markov processes [20], we derived, for all α , the joint probability distribution of $M(t)$ and $t_m(t)$. Marginalising this joint distribution for $M(t)$ shows that the distribution $\mathcal{P}_m(M|t)$ possesses scaling behaviour in $M/t^{\frac{1}{2+\alpha}}$ with the corresponding scaling function $\mathcal{F}_\alpha(z)$ rigorously derived in Eq. (9). Contrary to the standard Brownian motion

(SBm), we obtain that $\mathcal{F}_\alpha(z)$, for non-zero α , has a non-monotonic dependence on z . Our analysis also provides an exact expression of the marginal distribution $\mathcal{P}_m(t_m|t)$ of the arg-maximum $t_m(t)$. In particular, for non-zero α , we see that this distribution is not symmetric about $t_m = t/2$ and possesses different peaks (divergences) as $t_m \rightarrow 0^+$ and $t_m \rightarrow t^-$, namely, $\mathcal{P}_m(t_m \rightarrow 0|t) \sim t_m^{-\frac{1+\alpha}{2+\alpha}}$ and $\mathcal{P}_m(t_m \rightarrow t|t) \sim (t - t_m)^{-\frac{1}{2}}$. This behaviour is in sharp contrast with respect to the SBm ($\alpha = 0$) for which $\mathcal{P}_m(t_m|t)$ is symmetric about $t_m = t/2$ and diverges identically as $\mathcal{P}_m(t_m \rightarrow 0|t) \sim t_m^{-\frac{1}{2}}$ and $\mathcal{P}_m(t_m \rightarrow t|t) \sim (t - t_m)^{-\frac{1}{2}}$.

The second part of our paper dealt with the analysis of residence time $t_r(t)$ for which we computed the probability distribution $\mathcal{P}_r(t_r|t)$ exactly for all values of α . Quite remarkably, we find the existence of a critical α (which we denote by $\alpha_c = -0.3182$) such that $\mathcal{P}_r(t_r|t)$ has minima at $t_r = t/2$ for $\alpha \geq \alpha_c$ whereas it exhibits local maximum at $t_r = t/2$ for $\alpha < \alpha_c$. We provide a simple physical reasoning of this behaviour based on the likelihood of the particle to stay on one side of the origin. Finally, we calculated the distribution $\mathcal{P}_\ell(t_\ell|t)$ of the last-passage time $t_\ell(t)$ and showed that it is also asymmetric about $t_\ell(t) = t/2$ for non-zero α . This is further exemplified by the difference in behaviour of $\mathcal{P}_\ell(t_\ell|t)$ as $t_\ell \rightarrow 0^+$ and $t_\ell \rightarrow t^-$, viz. $\mathcal{P}_\ell(t_\ell \rightarrow 0|t) \sim t_\ell^{-\frac{1+\alpha}{2+\alpha}}$ and $\mathcal{P}_\ell(t_\ell \rightarrow t|t) \sim (t - t_\ell)^{-\frac{1}{2+\alpha}}$. We emphasize that while the distributions of $t_m(t)$, $t_r(t)$ and $t_\ell(t)$ are all identical for $\alpha = 0$ [19], they turn out to be significantly different for $\alpha \neq 0$. In fact, for $\alpha = 0$ (SBm), the equivalence between $t_m(t)$ and $t_\ell(t)$ can be established based on the reflection property, inversion symmetry and time reversal symmetry [93]. However, these symmetries are not present for $\alpha \neq 0$ which results in inequivalence between $t_m(t)$ and $t_\ell(t)$.

Here, we have showcased a simple example of heterogeneous diffusion model for which we could derive many results on extremal statistics and path functionals exactly. Unravelling these results for other complex heterogeneous models remains a promising future direction. Recently heterogeneous diffusion processes driven by coloured noise have garnered significant interest due to their potential application in biological systems [15–17]. It would be interesting to see how our results get modified in these scenarios.

VII. ACKNOWLEDGEMENT

I am indebted to my supervisor Dr. Anupam Kundu for collaboration on other projects upon which the current work is based. I acknowledge support of the Department of Atomic Energy, Government of India, under project no.12-R&D-TFR-5.10-1100.

Appendix A: Derivation of $\bar{S}_M(s|x_0)$

In this appendix, we derive the expression of $\bar{S}_M(s|x_0)$ written in Eq. (25). To this aim, we begin with the backward Fokker Planck equation (24) and perform the transformation

$$\bar{S}_M(s|x_0) = \frac{1}{s} + U(x_0). \quad (\text{A1})$$

This results in a homogeneous differential equation of the form

$$sU(x_0) = D(x_0)\partial_{x_0}^2 U(x_0), \quad (\text{A2})$$

with $D(x_0)$ defined in Eq. (6). Recall that $0 \leq M \leq \infty$ and $-\infty \leq x_0 \leq M$. We proceed to solve Eq. (A2) separately for $x_0 > 0$ and $x_0 < 0$ regions. For $x_0 > 0$, we perform the transformation $y = \frac{x_0^{2+\alpha}}{(2+\alpha)2l^\alpha D_0}$ and rewrite Eq. (A2) as

$$y \frac{\partial^2 U}{\partial y^2} + \left(\frac{1+\alpha}{2+\alpha} \right) \frac{\partial U}{\partial y} = sU. \quad (\text{A3})$$

The solution of this equation is given in terms of the modified Bessel functions as

$$U(y) = \mathbb{C}_1 y^{\frac{1}{2(2+\alpha)}} K_{\frac{1}{2+\alpha}}(2\sqrt{sy}) + \mathbb{C}_2 y^{\frac{1}{2(2+\alpha)}} I_{\frac{1}{2+\alpha}}(2\sqrt{sy}). \quad (\text{A4})$$

Here \mathbb{C}_1 and \mathbb{C}_2 are constants independent of y . Writing this solution in terms of x_0 and using Eq. (A1) to write $\bar{S}_M(s|x_0)$ in terms of $U(x_0)$, we get

$$\begin{aligned} \bar{S}_M(s|x_0) &= \frac{1}{s} + \mathbb{C}_1 \sqrt{x_0} K_{\frac{1}{2+\alpha}} \left((a_s x_0)^{\frac{2+\alpha}{2}} \right) \\ &\quad + \mathbb{C}_2 \sqrt{x_0} I_{\frac{1}{2+\alpha}} \left((a_s x_0)^{\frac{2+\alpha}{2}} \right). \end{aligned} \quad (\text{A5})$$

where a_s is given in Eq. (27). Recall that the solution in Eq. (A5) is true only for $x_0 > 0$. Proceeding similarly for $x_0 < 0$ yields

$$\begin{aligned} \bar{S}_M(s|x_0) &= \frac{1}{s} + \mathbb{C}_3 \sqrt{|x_0|} K_{\frac{1}{2+\alpha}} \left((a_s |x_0|)^{\frac{2+\alpha}{2}} \right) \\ &\quad + \mathbb{C}_4 \sqrt{|x_0|} I_{\frac{1}{2+\alpha}} \left((a_s |x_0|)^{\frac{2+\alpha}{2}} \right). \end{aligned} \quad (\text{A6})$$

The task is now to evaluate the constants \mathbb{C}_1 , \mathbb{C}_2 , \mathbb{C}_3 and \mathbb{C}_4 which are, in principle, functions of s . To compute them, we first note that the survival probability $S_M(t|x_0)$ and its derivative $\partial_{x_0} S_M(t|x_0)$ are continuous across $x_0 = 0$ which implies that $\bar{S}_M(s|x_0)$ and $\partial_{x_0} \bar{S}_M(s|x_0)$ are also continuous. This implies

$$\bar{S}_M(s|x_0 \rightarrow 0^+) = \bar{S}_M(s|x_0 \rightarrow 0^-), \quad (\text{A7})$$

$$\left[\frac{\partial \bar{S}_M(s|x_0)}{\partial x_0} \right]_{x_0 \rightarrow 0^+} = \left[\frac{\partial \bar{S}_M(s|x_0)}{\partial x_0} \right]_{x_0 \rightarrow 0^-}. \quad (\text{A8})$$

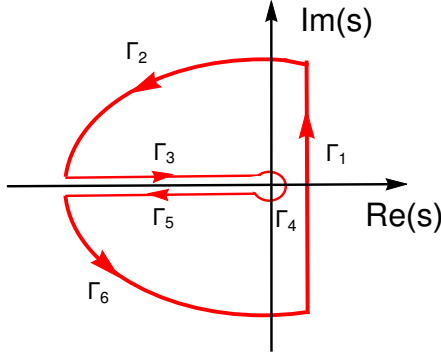


FIG. 7. Contour for the Bromwich integration of $\bar{J}(M, s)$ in Eq. (34)

Next, we recall the boundary conditions of $S_M(t|x_0)$ in Eqs. (22) and (23). Translating these conditions in terms of $\bar{S}_M(s|x_0)$ yields

$$\bar{S}_M(s|x_0 \rightarrow M) = 0, \quad (\text{A9})$$

$$\bar{S}_M(s|x_0 \rightarrow -\infty) = \frac{1}{s}. \quad (\text{A10})$$

Using the four conditions [Eqs. (A7)-(A10)], we obtain the constants \mathbb{C}_1 , \mathbb{C}_2 , \mathbb{C}_3 and \mathbb{C}_4 . This completely specifies the Laplace transform $\bar{S}_M(s|x_0)$ in Eqs. (A5) and (A6). However, since we are eventually interested in computing the joint distribution of the maximum $M(t)$ and arg-max $t_m(t)$, we provide the solution only for $x_0 \geq 0$. As evident from Eq. (A5), we then need only the expressions of \mathbb{C}_1 and \mathbb{C}_2 which read

$$\mathbb{C}_1 = \frac{\mathbb{C}_2}{\Gamma\left(\frac{1}{2+\alpha}\right)\Gamma\left(\frac{1+\alpha}{2+\alpha}\right)}, \quad (\text{A11})$$

$$\mathbb{C}_2 = -\frac{1}{sf_\alpha(M)}, \quad \text{with}, \quad (\text{A12})$$

$$f_\alpha(M) = \frac{1}{2\sqrt{a_s}} \mathcal{H}_{\frac{1}{2+\alpha}}\left((a_s M)^{\frac{2+\alpha}{2}}\right), \quad (\text{A13})$$

where $\mathcal{H}_\beta(x_0)$ in the last equation is given in Eq. (26). Finally, inserting these expressions in Eq. (A5), we find

$$\bar{S}_M(s|x_0) = \frac{1}{s} \left[1 - \frac{\mathcal{H}_{\frac{1}{2+\alpha}}\left((a_s x_0)^{\frac{2+\alpha}{2}}\right)}{\mathcal{H}_{\frac{1}{2+\alpha}}\left((a_s M)^{\frac{2+\alpha}{2}}\right)} \right], \quad (\text{A14})$$

which has been written in Eq. (25) in the main text.

Appendix B: Inverse Laplace transformation of $\bar{P}_m(M|s)$

Here, we perform the inverse Laplace transformation of $\bar{P}_m(M|s)$ in Eq. (33) to obtain the distribution $P_m(M|t)$ quoted in Eq. (8). Since from Eq. (33), we observe that

$\bar{P}_m(M|s)$ is simply the derivative of $\bar{J}(M, s)$, we therefore look at the inverse Laplace transformation of $\bar{J}(M, s)$ in Eq. (34). We will then use this to compute the marginal distribution $P_m(M|t)$.

Denoting the inverse Laplace transform of $\bar{J}(M, s)$ by $J(M, t)$, we have

$$J(M, t) = \frac{1}{2\pi i} \int_{-i\infty}^{i\infty} ds e^{st} \bar{J}(M, s), \quad (\text{B1})$$

$$= \frac{\mathcal{H}_{\frac{1}{2+\alpha}}(0)}{2\pi i} \int_{-i\infty}^{i\infty} ds \frac{e^{st}}{s \mathcal{H}_{\frac{1}{2+\alpha}}\left(\sqrt{\frac{sM^{2+\alpha}}{\mathcal{D}_\alpha}}\right)}. \quad (\text{B2})$$

Notice that $s = 0$ is a branch point. To perform this Bromwich integration, we consider the contour of form shown in Figure 7. Since the integrand is analytic inside this contour, the Cauchy theorem gives

$$\int_{\Gamma_1} + \int_{\Gamma_2} + \int_{\Gamma_3} + \int_{\Gamma_4} + \int_{\Gamma_5} + \int_{\Gamma_6} = 0. \quad (\text{B3})$$

$\int_{\Gamma_1} = J(M, t)$ is the integral that we need. Recall that the real part of s along Γ_2 and Γ_6 is negative and in the limit $|s| \rightarrow \infty$, the contribution becomes exactly zero.

To evaluate integral along Γ_3 , we substitute $s = Re^{i\pi}$, where R varies from ∞ to 0. With this transformation, \int_{Γ_3} becomes

$$\int_{\Gamma_3} = \frac{\mathcal{H}_{\frac{1}{2+\alpha}}(0)}{2\pi i} \int_{\infty}^0 dR \frac{e^{-Rt}}{R \mathcal{H}_{\frac{1}{2+\alpha}}\left(i\sqrt{\frac{RM^{2+\alpha}}{\mathcal{D}_\alpha}}\right)}. \quad (\text{B4})$$

Substituting $w = \frac{RM^{2+\alpha}}{\mathcal{D}_\alpha}$, we get

$$\int_{\Gamma_3} = -\frac{\mathcal{H}_{\frac{1}{2+\alpha}}(0)}{2\pi i} \int_0^{\infty} dw \frac{e^{-\frac{\mathcal{D}_\alpha t}{M^{2+\alpha}} w}}{w \mathcal{H}_{\frac{1}{2+\alpha}}(i\sqrt{w})}. \quad (\text{B5})$$

Next, we evaluate the integral along Γ_5 . For this, we substitute $s = e^{-i\pi}R$ in the integrand and perform similar simplifications as done for Γ_3 . We then obtain

$$\int_{\Gamma_5} = \frac{\mathcal{H}_{\frac{1}{2+\alpha}}(0)}{2\pi i} \int_0^{\infty} dw \frac{e^{-\frac{\mathcal{D}_\alpha t}{M^{2+\alpha}} w}}{w \mathcal{H}_{\frac{1}{2+\alpha}}(-i\sqrt{w})}. \quad (\text{B6})$$

Finally, we perform the integration along Γ_4 for which we replace $s = \delta e^{i\theta}$ and take $\delta \rightarrow 0^+$ limit. It is easy to show that the resultant integration is $\int_{\Gamma_4} = -1$.

Putting all the intergations together and noting $\int_{\Gamma_1} = J(M, t)$, we use Eq. (B3) to write $J(M, t)$ as

$$J(M, t) = -\int_{\Gamma_3} - \int_{\Gamma_4} - \int_{\Gamma_5}, \quad (\text{B7})$$

$$= 1 - \frac{\mathcal{H}_{\frac{1}{2+\alpha}}(0)}{(2+\alpha)} \int_0^{\infty} \frac{dw}{w} e^{-\frac{\mathcal{D}_\alpha t}{M^{2+\alpha}} w} \mathbb{H}_{\frac{1}{2+\alpha}}(\sqrt{w}), \quad (\text{B8})$$

where the function $\mathbb{H}_\beta(w)$ is given by

$$\mathbb{H}_\beta(w) = \frac{1}{2\pi\beta i} \left[\frac{1}{\mathcal{H}_\beta(-iw)} - \frac{1}{\mathcal{H}_\beta(iw)} \right]. \quad (\text{B9})$$

Coming back to the inverse Laplace transform of $\bar{P}_m(M|s)$, we use Eq. (33) to write $P_m(M|t)$ in terms of $J(M, t)$ as

$$P_m(M|t) = -\frac{dJ(M, t)}{dM}. \quad (\text{B10})$$

Inserting $J(M, t)$ from Eq. (B8) in Eq. (B10) yields

$$P_m(M|t) = \frac{1}{(\mathcal{D}_\alpha t)^{\frac{1}{2+\alpha}}} \mathcal{F}_\alpha \left(\frac{M}{(\mathcal{D}_\alpha t)^{\frac{1}{2+\alpha}}} \right), \quad (\text{B11})$$

where \mathcal{D}_α and $\mathcal{F}_\alpha(z)$ are, respectively, given in Eqs. (27) and (9).

Appendix C: Asymptotic behaviour of the scaling function $\mathcal{F}_\alpha(z)$

This appendix deals with the derivation of the asymptotic behaviour of the scaling function $\mathcal{F}_\alpha(z)$ which are quoted in Eqs. (37) and (38). For simplicity, we look at the small and large z behaviours separately below.

1. Small z behaviour of $\mathcal{F}_\alpha(z)$

To obtain $\mathcal{F}_\alpha(z \rightarrow 0)$, we consider the form of $\bar{P}(M|s)$ in terms of $\bar{J}(M, s)$ as shown in Eq. (33) and look at the small M behaviour of $\bar{J}(M, s)$. As evident from Eq. (34), one then needs to specify the small- x form of $\mathcal{H}_\beta(x)$. For $x \rightarrow 0$, the modified Bessel function is

$$I_\beta(x) \simeq \frac{x^\beta}{2^\beta \Gamma(1+\beta)} + \frac{x^{2+\beta}}{2^{2+\beta} \Gamma(2+\beta)}, \quad (\text{C1})$$

which we use in Eq. (26) to get

$$\mathcal{H}_\beta(x) \simeq \mathcal{H}_\beta(0) + \frac{x^{2\beta}}{2^\beta \Gamma(1+\beta)}, \quad \text{as } x \rightarrow 0. \quad (\text{C2})$$

Substituting this expression in $\bar{J}(M, s)$ in Eq. (34) for $M \rightarrow 0$, we get

$$\bar{J}(M, s) \simeq \frac{C_\alpha \mathcal{D}_\alpha^{\frac{1}{2+\alpha}}}{s \left(C_\alpha \mathcal{D}_\alpha^{\frac{1}{2+\alpha}} + M s^{\frac{1}{2+\alpha}} \right)}, \quad (\text{C3})$$

with $C_\alpha = \frac{2^{2/2+\alpha} \Gamma(\frac{1}{2+\alpha})}{(2+\alpha) \Gamma(\frac{1}{2+\alpha})}$. Next, we insert Eq. (C3) in Eq. (33) to yield the small- M behaviour of $\bar{P}_m(M|s)$ for $\alpha \neq 0$ as

$$\bar{P}_m(M|s) \simeq \frac{1}{C_\alpha \mathcal{D}_\alpha^{\frac{1}{2+\alpha}} s^{\frac{1+\alpha}{2+\alpha}}} - \frac{2M}{C_\alpha^2 \mathcal{D}_\alpha^{\frac{2}{2+\alpha}} s^{\frac{\alpha}{2+\alpha}}}. \quad (\text{C4})$$

Finally, we perform the inverse Laplace transformation and obtain

$$P_m(M|t) = \frac{1}{(\mathcal{D}_\alpha t)^{\frac{1}{2+\alpha}}} \mathcal{F}_\alpha \left(\frac{M}{(\mathcal{D}_\alpha t)^{\frac{1}{2+\alpha}}} \right), \quad (\text{C5})$$

where the scaling function $\mathcal{F}_\alpha(z)$ has the form

$$\mathcal{F}_\alpha(z \rightarrow 0) \simeq \frac{1}{C_\alpha \Gamma\left(\frac{1+\alpha}{2+\alpha}\right)} - \frac{2z}{C_\alpha^2 \Gamma\left(\frac{\alpha}{2+\alpha}\right)}, \quad \text{for } \alpha \neq 0. \quad (\text{C6})$$

On the other hand, for $\alpha = 0$, we saw that $\mathcal{F}_\alpha(z) = \frac{e^{-z^2/4}}{\sqrt{\pi}}$ which for small z becomes

$$\mathcal{F}_\alpha(z \rightarrow 0) \simeq \frac{1}{\sqrt{\pi}} \left(1 - \frac{z^2}{4} \right), \quad \text{for } \alpha = 0. \quad (\text{C7})$$

Eqs. (C6) and (C7) completely specifies the small- z behaviour of $\mathcal{F}_\alpha(z)$ for all values of α .

2. Large z behaviour of $\mathcal{F}_\alpha(z)$

We next look at the large- z behaviour of $\mathcal{F}_\alpha(z)$. Once again, we use Eq. (33) and analyse $\bar{J}(M, s)$ for large M . Using the asymptotic expression of modified Bessel function for large x as

$$I_\beta(x) \simeq \frac{e^x}{\sqrt{2\pi x}}, \quad (\text{C8})$$

we use Eq. (26) to get $\mathcal{H}_\beta(x)$

$$\mathcal{H}_\beta(x) \simeq \sqrt{\frac{2}{\pi}} \frac{e^x}{x^{\frac{1}{2}-\beta}}, \quad \text{as } x \rightarrow \infty. \quad (\text{C9})$$

Substituting this in the expression of $\bar{J}(M, s)$ in Eq. (34), we find

$$\bar{J}(M, s) \simeq \frac{\mathcal{H}_{\frac{1}{2+\alpha}}(0)}{s} \sqrt{\frac{\pi}{2}} (a_s M)^{\frac{\alpha}{4}} e^{-(a_s M)^{\frac{2+\alpha}{2}}}. \quad (\text{C10})$$

as $M \rightarrow \infty$. Inserting this in $\bar{P}_m(M|s)$ in Eq. (33) and performing some algebraic simplifications gives

$$\bar{P}_m(M|s) \simeq \frac{Z_\alpha}{s^{\frac{4+\alpha}{4(2+\alpha)}}} \exp(-2b_M \sqrt{s}), \quad \text{as } M \rightarrow \infty, \quad (\text{C11})$$

where b_M and Z_α are defined as

$$b_M = \frac{1}{2} \sqrt{\frac{M^{2+\alpha}}{\mathcal{D}_\alpha}}, \quad (\text{C12})$$

$$Z_\alpha = \frac{(2+\alpha)\sqrt{\pi}}{2\sqrt{2}} \left(\frac{M^{\frac{3\alpha}{4}} \mathcal{H}_{\frac{1}{2+\alpha}}(0)}{\mathcal{D}_\alpha^{\frac{4+3\alpha}{4(2+\alpha)}}} \right). \quad (\text{C13})$$

We now proceed to perform the inverse Laplace transformation of $\bar{P}_m(M|s)$ in Eq. (C11). To this end, we exploit the convolution property of Laplace transformation to write

$$P_m(M|t) \simeq Z_\alpha \int_0^t dT \mathcal{L}_{s \rightarrow t-T} \left[\frac{1}{s^{\frac{4+\alpha}{4(2+\alpha)}}} \right] \times \mathcal{L}_{s \rightarrow T} [\exp(-2b_M \sqrt{s})], \quad (\text{C14})$$

where the notation $\mathcal{L}_{s \rightarrow t}$ denoted the inverse Laplace transformation as indicated in Eq. (18). Using the inverse Laplace transformations

$$\mathcal{L}_{s \rightarrow t} [\exp(-2b_M \sqrt{s})] = \frac{b_M}{\sqrt{\pi t^3}} e^{-\frac{b_M^2}{t}}, \quad (\text{C15})$$

$$\mathcal{L}_{s \rightarrow t} \left[s^{-\frac{4+\alpha}{4(2+\alpha)}} \right] = \frac{t^{\frac{4+\alpha}{4(2+\alpha)}-1}}{\Gamma\left(\frac{4+\alpha}{4(2+\alpha)}\right)}, \quad (\text{C16})$$

in Eq. (C14), we find

$$P_m(M|t) \simeq \frac{Z_\alpha M^{\frac{2+\alpha}{2}} \mathbb{I}\left(\frac{M^{2+\alpha}}{4\mathcal{D}_\alpha t}\right)}{\sqrt{4\pi\mathcal{D}_\alpha} \Gamma\left(\frac{4+\alpha}{8+4\alpha}\right) t^{\frac{8+5\alpha}{8+4\alpha}}}, \quad (\text{C17})$$

where the function $\mathbb{I}(y)$ is defined as

$$\mathbb{I}(y) = \int_0^1 dw \frac{e^{-y/w}}{w^{3/2}(1-w)^{\frac{4+3\alpha}{8+4\alpha}}}, \quad y > 0. \quad (\text{C18})$$

As seen in Eq. (C17), we need to evaluate $\mathbb{I}\left(\frac{M^{2+\alpha}}{4\mathcal{D}_\alpha t}\right)$ for large M . In appendix C3, we have shown that the asymptotic expression of the function $\mathbb{I}(y)$ is

$$\mathbb{I}(y) \simeq \frac{e^{-y}}{y^{\frac{4+\alpha}{8+4\alpha}}} \Gamma\left(\frac{4+\alpha}{8+4\alpha}\right), \quad \text{as } y \rightarrow \infty. \quad (\text{C19})$$

Finally, substituting this in Eq. (C17), we find

$$P_m(M|t) = \frac{1}{(\mathcal{D}_\alpha t)^{\frac{1}{2+\alpha}}} \mathcal{F}_\alpha \left(\frac{M}{(\mathcal{D}_\alpha t)^{\frac{1}{2+\alpha}}} \right), \quad (\text{C20})$$

with the scaling function given by

$$\mathcal{F}_\alpha(z \rightarrow \infty) \simeq \frac{(2+\alpha)\mathcal{H}_{\frac{1}{2+\alpha}}(0)}{2^{\frac{3+2\alpha}{2+\alpha}}} z^\alpha e^{-\frac{z^{2+\alpha}}{4}}. \quad (\text{C21})$$

This expression has been quoted in Eq. (38) in the main text.

3. $\mathbb{I}(y)$ in Eq. (C18) as $y \rightarrow \infty$

Here, we evaluate the asymptotic form of $\mathbb{I}(y)$ in Eq. (C19) as $y \rightarrow \infty$ which was used to compute $P_m(M|t)$

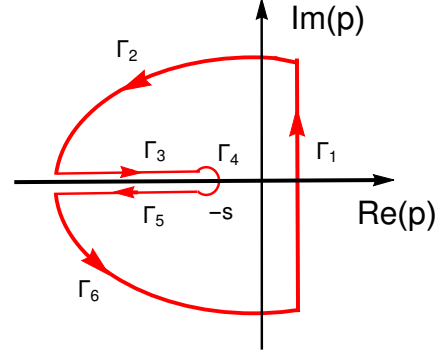


FIG. 8. Contour for the Bromwich integration of $\bar{\mathbb{Y}}_\alpha(s, p, w)$ in Eq. (D2)

for large M . For this, we first replace $w = \bar{w}^{-1}$ in Eq. (C18) and rewrite

$$\mathbb{I}(y) = \int_1^\infty \frac{d\bar{w}}{\bar{w}^{\frac{\alpha}{8+4\alpha}}} \frac{e^{-y\bar{w}}}{(\bar{w}-1)^{\frac{4+3\alpha}{8+4\alpha}}}. \quad (\text{C22})$$

For $y \rightarrow \infty$, the integral will be dominated by small values of \bar{w} which in the given domain of integration is equal to 1. Consequently, we get

$$\mathbb{I}(y \rightarrow \infty) \simeq \int_1^\infty d\bar{w} \frac{e^{-y\bar{w}}}{(\bar{w}-1)^{\frac{4+3\alpha}{8+4\alpha}}}. \quad (\text{C23})$$

Finally, changing the variable $\bar{w} = w + 1$, we get

$$\mathbb{I}(y \rightarrow \infty) \simeq e^{-y} \int_0^\infty dw \frac{e^{-yw}}{w^{\frac{4+3\alpha}{8+4\alpha}}}, \quad (\text{C24})$$

$$\simeq \frac{e^{-y}}{y^{\frac{4+\alpha}{8+4\alpha}}} \Gamma\left(\frac{4+\alpha}{8+4\alpha}\right). \quad (\text{C25})$$

Appendix D: Inverse Laplace transformation of $\bar{\mathcal{P}}_m(p|s)$

In this appendix, we will perform the double inverse Laplace transformation of $\bar{\mathcal{P}}_m(p|s)$ in Eq. (42) to obtain the distribution $\mathcal{P}_m(t_m|t)$ in time domain. As evident from Eq. (42), we then need to compute the inverse Laplace transformation of $\bar{\mathbb{Y}}_\alpha(s, p, w)$. Then $\mathcal{P}_m(t_m|t)$ is given as

$$\mathcal{P}_m(t_m|t) = \frac{\mathcal{H}_{\frac{1}{2+\alpha}}(0)}{2(2+\alpha)^{-1}} \int_0^\infty dw \frac{\mathbb{Y}_\alpha(t, t_m, w)}{\mathcal{H}_{\frac{1}{2+\alpha}}\left(w^{\frac{2+\alpha}{2}}\right)}, \quad (\text{D1})$$

where $\mathbb{Y}_\alpha(t, t_m, w)$ is the double inverse Laplace transformation of $\bar{\mathbb{Y}}_\alpha(s, p, w)$:

$$\mathbb{Y}_\alpha(t, t_m, w) = \mathcal{L}_{s \rightarrow t} \mathcal{L}_{p \rightarrow t_m} [\bar{\mathbb{Y}}_\alpha(s, p, w)]. \quad (\text{D2})$$

We proceed to perform inversion first with respect to p for which we use Eq. (18) and write the Bromwich integral as

$$\mathbb{E}(s, t_m, w) = \mathcal{L}_{p \rightarrow t_m} [\bar{\mathbb{Y}}_\alpha(s, p, w)], \quad (\text{D3})$$

$$= \frac{1}{2\pi i} \int_{-i\infty}^{i\infty} dp e^{pt_m} \bar{\mathbb{Y}}_\alpha(s, p, w). \quad (\text{D4})$$

Note that the integrand $\bar{\mathbb{Y}}_\alpha(s, p, w)$ has a branch point at $p = -s$ [see Eq. (43)]. To perform this complex integration, we consider contour shown in Figure 8. Since $\bar{\mathbb{Y}}_\alpha(s, p, w)$ is analytic inside this contour, the Cauchy theorem gives

$$\int_{\Gamma_1} + \int_{\Gamma_2} + \int_{\Gamma_3} + \int_{\Gamma_4} + \int_{\Gamma_5} + \int_{\Gamma_6} = 0. \quad (\text{D5})$$

Here \int_{Γ_1} is the integration that we need. Let us calculate the integrations across various paths in Eq. (D5). Note that the real part of p is negative along paths Γ_2 and Γ_6 and in the limit $|p| \rightarrow \infty$, the integrand becomes exactly zero. Hence, the contribution of these two paths is equal to zero.

Along Γ_4 , we replace $p = -s + \delta e^{i\theta}$ and take limit $\delta \rightarrow 0^+$. For small δ , we find that the integrand scales as $\sim \sqrt{\delta}$ which vanishes as $\delta \rightarrow 0^+$. Hence, the contribution of this path is also zero.

Next, we look at the contribution of Γ_3 . For this path, we replace $p = -s + Re^{i\pi}$ and perform some algebraic simplifications to get

$$\int_{\Gamma_3} = \frac{w^{1+\alpha} e^{-\frac{i\pi}{2+\alpha}}}{2\pi i} \int_0^\infty du \frac{e^{-(1+uw^{2+\alpha})st_m} \mathcal{H}_{\frac{1+\alpha}{2+\alpha}}\left(-\frac{i}{\sqrt{u}}\right)}{u^{\frac{1}{2+\alpha}} \mathcal{H}_{\frac{1}{2+\alpha}}\left(-\frac{i}{\sqrt{u}}\right)}.$$

Similarly, for Γ_5 , we replace $p = -s + Re^{-i\pi}$ and proceed exactly as before to get

$$\int_{\Gamma_5} = -\frac{w^{1+\alpha} e^{\frac{i\pi}{2+\alpha}}}{2\pi i} \int_0^\infty du \frac{e^{-(1+uw^{2+\alpha})st_m} \mathcal{H}_{\frac{1+\alpha}{2+\alpha}}\left(\frac{i}{\sqrt{u}}\right)}{u^{\frac{1}{2+\alpha}} \mathcal{H}_{\frac{1}{2+\alpha}}\left(\frac{i}{\sqrt{u}}\right)}.$$

Plugging all these contribution in Eq. (D5) and noting $\int_{\Gamma_1} = \mathbb{E}(s, t_m, w)$, we find

$$\mathbb{E}(s, t_m, w) = \int_0^\infty du \frac{w^{1+\alpha} e^{-(1+uw^{2+\alpha})st_m}}{u^{\frac{1}{2+\alpha}}} \mathbb{X}_\alpha(\sqrt{u}), \quad (\text{D6})$$

where the function $\mathbb{X}_\alpha(u)$ is defined as

$$\mathbb{X}_\alpha(u) = \frac{e^{\frac{i\pi}{2+\alpha}}}{2\pi i} \left[\frac{\mathcal{H}_{\frac{1+\alpha}{2+\alpha}}\left(\frac{i}{\sqrt{u}}\right)}{\mathcal{H}_{\frac{1}{2+\alpha}}\left(\frac{i}{\sqrt{u}}\right)} - \frac{e^{-\frac{2i\pi}{2+\alpha}} \mathcal{H}_{\frac{1+\alpha}{2+\alpha}}\left(-\frac{i}{\sqrt{u}}\right)}{\mathcal{H}_{\frac{1}{2+\alpha}}\left(-\frac{i}{\sqrt{u}}\right)} \right]. \quad (\text{D7})$$

Inserting $\mathbb{E}(s, t_m, w)$ from Eq. (D6) in $\mathbb{Y}_\alpha(t, t_m, w)$ in Eq. (D2) and performing the inversion with s , we get

$$\mathbb{Y}_\alpha(t, t_m, w) = \frac{\mathbb{X}_\alpha\left(\sqrt{\frac{t-t_m}{t_m w^{2+\alpha}}}\right)}{t_m^{\frac{1+\alpha}{2+\alpha}} (t-t_m)^{\frac{1}{2+\alpha}}}. \quad (\text{D8})$$

Finally, substituting this form of $\mathbb{Y}_\alpha(t, t_m, w)$ in Eq. (D1) results in the expression of $\mathcal{P}_m(t_m|t)$ as written in Eq. (10).

Appendix E: Asymptotic form of $\mathcal{G}_m^\alpha(z)$

Here, we analyse the asymptotic behaviour of the scaling function $\mathcal{G}_m^\alpha(z)$ in Eq. (11) as $z \rightarrow 0$ and $z \rightarrow 1$. For clarity, we present this analysis separately for $z \rightarrow 0$ and $z \rightarrow 1$.

1. $\mathcal{G}_m^\alpha(z)$ as $z \rightarrow 0$

Looking at the expression of $\mathcal{G}_m^\alpha(z)$ in Eq. (11), we see that one needs to specify the behaviour of $\mathbb{X}_\alpha\left(\sqrt{\frac{1-z}{z w^{2+\alpha}}}\right)$ as $z \rightarrow 0$. To this end, we use the expression of $\mathbb{X}_\alpha(x)$ in Eq. (D7) as $x \rightarrow \infty$ which reads

$$\mathbb{X}_\alpha(x \rightarrow \infty) \simeq \frac{\sin\left(\frac{\pi}{2+\alpha}\right) \mathcal{H}_{\frac{1+\alpha}{2+\alpha}}(0)}{\pi \mathcal{H}_{\frac{1}{2+\alpha}}(0)}. \quad (\text{E1})$$

Plugging this in Eq. (11), we see that

$$\mathcal{G}_m^\alpha(z) \sim z^{-\frac{1+\alpha}{2+\alpha}}, \quad \text{as } z \rightarrow 0. \quad (\text{E2})$$

2. $\mathcal{G}_m^\alpha(z)$ as $z \rightarrow 1$

Once again, we use the expression $\mathcal{G}_m^\alpha(z)$ in Eq. (11). As evident from this equation, one then needs to specify the small- x behaviour of $\mathbb{X}_\alpha(x)$. Using $\mathcal{H}_\beta(u \rightarrow \infty) \simeq \sqrt{\frac{1}{\pi}} e^u u^{\beta-\frac{1}{2}}$ in Eq. (D7), it is easy to show that

$$\mathbb{X}_\alpha(x \rightarrow 0) \simeq \frac{1}{\pi x^{\frac{\alpha}{2+\alpha}}}. \quad (\text{E3})$$

Inserting this in Eq. (11) yields

$$\mathcal{G}_m^\alpha(z) \sim (1-z)^{-\frac{1}{2}}, \quad \text{as } z \rightarrow 1. \quad (\text{E4})$$

Appendix F: Residence time distribution $\mathcal{P}_r(t_r|t)$

Here we will solve the backward master equation (46) to get the probability distribution of the residence time $t_r(t)$. For this, we first take the Laplace transformation of Eq. (46) with respect to t and rewrite it as

$$[s + p \Theta(x_0)] \bar{\mathcal{Q}}(p, x_0|s) - 1 = D(x_0) \partial_{x_0}^2 \bar{\mathcal{Q}}(p, x_0|s), \quad (\text{F1})$$

where $\bar{\mathcal{Q}}(p, x_0|s)$ is the Laplace transformation of $\mathcal{Q}(p, x_0|t)$. For $x_0 > 0$, this equation becomes

$$(s + p) \bar{\mathcal{Q}}(p, x_0|s) - 1 = D(x_0) \partial_{x_0}^2 \bar{\mathcal{Q}}(p, x_0|s). \quad (\text{F2})$$

To simplify this equation further, we make the following transformations:

$$y = \frac{x_0^{2+\alpha}}{(2+\alpha)^2 l^\alpha D_0}, \quad (\text{F3})$$

$$\bar{Q}(p, x_0|s) = \frac{1}{s+p} + Q(p, x_0|s), \quad (\text{F4})$$

and rewrite Eq. (F2) in terms of $Q(p, x_0|s)$ and y as

$$y \frac{\partial^2 Q}{\partial y^2} + \left(\frac{1+\alpha}{2+\alpha} \right) \frac{\partial Q}{\partial y} = (s+p)Q. \quad (\text{F5})$$

This equation can now be solved and its solutions are given in terms of the modified Bessel functions as $y^{\frac{1}{2(2+\alpha)}} I_{\frac{1}{2+\alpha}} \left(2\sqrt{(s+p)y} \right)$ and $y^{\frac{1}{2(2+\alpha)}} K_{\frac{1}{2+\alpha}} \left(2\sqrt{(s+p)y} \right)$. However, the former solution diverges in the limit $y \rightarrow \infty$. Hence, we consider only the later solution and write finally for $\bar{Q}(p, x_0|s)$ as

$$\bar{Q}(p, x_0|s) = \frac{1}{s+p} + \mathbb{C}_5 \sqrt{x} K_{\frac{1}{2+\alpha}} \left((a_{s+p} x_0)^{\frac{2+\alpha}{2}} \right), \quad (\text{F6})$$

where a_{s+p} is given in Eq. (27) and \mathbb{C}_5 is a function independent of y , but can, in principle, depend on s and p . Recall that the solution in Eq. (F6) holds only for $x_0 > 0$. Proceeding similarly for $x_0 < 0$, we get

$$\bar{Q}(p, x_0|s) = \frac{1}{s} + \mathbb{C}_6 \sqrt{x} K_{\frac{1}{2+\alpha}} \left((a_s |x_0|)^{\frac{2+\alpha}{2}} \right). \quad (\text{F7})$$

Once again \mathbb{C}_6 here is a function independent of y , but can, in principle, depend on s and p . Now the task is to compute these functions \mathbb{C}_5 and \mathbb{C}_6 in Eqs. (F6) and (F7). For this computation, we use the continuity of $\bar{Q}(p, x_0|s)$ and $\partial_{x_0} \bar{Q}(p, x_0|s)$ across $x_0 = 0$:

$$\bar{Q}(p, x_0 \rightarrow 0^+|s) = \bar{Q}(p, x_0 \rightarrow 0^-|s), \quad (\text{F8})$$

$$\left(\frac{\partial \bar{Q}(p, x_0|s)}{\partial x_0} \right)_{x_0 \rightarrow 0^+} = \left(\frac{\partial \bar{Q}(p, x_0|s)}{\partial x_0} \right)_{x_0 \rightarrow 0^-}. \quad (\text{F9})$$

Then using these forms of \mathbb{C}_5 and \mathbb{C}_6 in Eqs. (F6) and (F7), we obtain the expression of $\bar{Q}(p, x_0|s)$ for all x_0 . However, we are interested only in the situation where the particle starts initially from the origin. For this case, we have

$$\bar{Q}(p|s) = \frac{1}{s} - \frac{p}{s(s+p)} \left[1 + \left(\frac{s}{s+p} \right)^{\frac{1}{2+\alpha}} \right]^{-1}, \quad (\text{F10})$$

where we have used the short hand notation $\bar{Q}(p|s)$ for $\bar{Q}(p, x_0 = 0|s)$. This result has been quoted in Eq. (50) in the main text.

Appendix G: Derivation of $\bar{\mathcal{P}}_\ell(p|s)$

In this appendix, we will derive the expression of the Laplace transform $\bar{\mathcal{P}}_\ell(p|s)$ in Eq. (58). As evident

from Eq. (55), $\bar{\mathcal{P}}_\ell(p|s)$ can be expressed in terms of the Laplace transformations of the survival probability $\bar{S}_0(s|\epsilon)$ and free distribution $\bar{\mathbb{P}}(\epsilon, s+p|0)$. In what follows, we first compute these two quantities and then use them in Eq. (55) to calculate $\bar{\mathcal{P}}_\ell(p|s)$.

1. Computation of $\bar{\mathbb{P}}(\epsilon, s|0)$

Denoting the probability distribution to be at x at time t starting from the origin by $\mathbb{P}(x, t|0)$, we write the Fokker-Planck equation (Ito sense) for $\mathbb{P}(x, t|0)$ as

$$\partial_t \mathbb{P}(x, t|0) = \partial_x^2 [D(x)\mathbb{P}(x, t|0)], \quad (\text{G1})$$

where $D(x)$ is given in Eq. (6). Taking Laplace transformation of this equation gives

$$s\bar{\mathbb{P}}(x, s|0) - \delta(x) = \partial_x^2 [D(x)\bar{\mathbb{P}}(x, s|0)]. \quad (\text{G2})$$

For $x \neq 0$, we get rid of the delta function and obtain

$$s\bar{\mathbb{P}}(x, s|0) = \partial_x^2 [D(x)\bar{\mathbb{P}}(x, s|0)]. \quad (\text{G3})$$

Let us first analyse this differential equation for $x > 0$. To simplify Eq. (G3), we perform the transformations

$$y = \frac{x^{2+\alpha}}{(2+\alpha)^2 l^\alpha D_0}, \quad (\text{G4})$$

$$\mathbb{Z}_L(x, s) = D(x)\bar{\mathbb{P}}(x, s|0), \quad (\text{G5})$$

and rewrite it as

$$y \frac{\partial^2 \mathbb{Z}_L}{\partial y^2} + \left(\frac{1+\alpha}{2+\alpha} \right) \frac{\partial \mathbb{Z}_L}{\partial y} = s\mathbb{Z}_L. \quad (\text{G6})$$

One can now solve this equation exactly and write solutions in terms of the modified Bessel functions as $y^{\frac{1}{2(2+\alpha)}} I_{\frac{1}{2+\alpha}} (2\sqrt{sy})$ and $y^{\frac{1}{2(2+\alpha)}} K_{\frac{1}{2+\alpha}} (2\sqrt{sy})$. Note that the former solution diverges in the limit $y \rightarrow \infty$. Hence, we consider only the later solution and write finally $\bar{\mathbb{P}}(x, s|0)$ as

$$\bar{\mathbb{P}}(x, s|0) = \frac{\mathbb{C}_7 \sqrt{x}}{D(x)} K_{\frac{1}{2+\alpha}} \left((a_s x)^{\frac{2+\alpha}{2}} \right), \quad (\text{G7})$$

where a_s is given in Eq. (27) and \mathbb{C}_7 is a constant which, in principle, depends on s and α . Recall that the expression of $\bar{\mathbb{P}}(x, s|0)$ in Eq. (G10) is valid only for $x > 0$. To compute this for $x < 0$, we recall that the problem possesses $x \rightarrow -x$ symmetry in the infinite line. Consequently, the same solution also applies for $x < 0$ and we have

$$\bar{\mathbb{P}}(x, s|0) = \frac{\mathbb{C}_7 \sqrt{|x|}}{D(x)} K_{\frac{1}{2+\alpha}} \left((a_s |x|)^{\frac{2+\alpha}{2}} \right), \quad (\text{G8})$$

for all x . The task now is to compute the constant \mathbb{C}_7 . To compute it, we integrate Eq. (G2) with respect to x

from ζ to $-\zeta$ and take $\zeta \rightarrow 0^+$. This gives rise to the following condition:

$$\left(\frac{\partial [D(x)\bar{\mathbb{P}}(x, s|0)]}{\partial x} \right)_{0^+} - \left(\frac{\partial [D(x)\bar{\mathbb{P}}(x, s|0)]}{\partial x} \right)_{0^-} = -1. \quad (\text{G9})$$

We next insert $\bar{\mathbb{P}}(x, s|0)$ from Eq. (G8) in Eq. (G12) which results in \mathbb{C}_7 as

$$\mathbb{C}_7(s) = \frac{2^{\frac{1}{2+\alpha}}}{(2+\alpha)\Gamma\left(\frac{1+\alpha}{2+\alpha}\right)} a_s^{-\frac{1}{2}}. \quad (\text{G10})$$

Inserting this in Eq. (G8), we obtain the exact form of $\bar{\mathbb{P}}(x, s|0)$. Since, we are interested in $\bar{\mathbb{P}}(\epsilon, s|0)$ with $\epsilon \rightarrow 0$ for last passage time [see Eq. (55)], we provide below only the expression of $\bar{\mathbb{P}}(\epsilon, s|0)$:

$$\bar{\mathbb{P}}(\epsilon, s|0) \simeq \frac{\mathcal{A}_L(\epsilon)}{s^{\frac{1}{2+\alpha}}}, \quad (\text{G11})$$

where the function $\mathcal{A}_L(\epsilon)$ is defined as

$$\mathcal{A}_L(\epsilon) = \frac{2^{-\frac{\alpha}{2+\alpha}} \mathcal{D}_\alpha \Gamma\left(\frac{1}{2+\alpha}\right)}{D(\epsilon)(2+\alpha)\Gamma\left(\frac{1+\alpha}{2+\alpha}\right)}. \quad (\text{G12})$$

We have quoted this result in Eq. (56) in the main text.

2. Computation of $\bar{S}_0(s|\epsilon)$

We now calculate $\bar{S}_0(s|\epsilon)$ which is essential for computing $\mathcal{P}_\ell(p|s)$ in Eq. (55). To compute $\bar{S}_0(s|\epsilon)$, we proceed exactly as in appendix A. In order to avoid the repetition, we present only the final result here.

$$\bar{S}_0(s|\epsilon) \simeq \frac{\mathcal{B}_L(\epsilon)}{s^{\frac{1+\alpha}{2+\alpha}}}, \quad (\text{G13})$$

where the function $\mathcal{B}_L(\epsilon)$ is defined as

$$\mathcal{B}_L(\epsilon) = \frac{\epsilon(2+\alpha)\Gamma\left(\frac{1+\alpha}{2+\alpha}\right)}{(4\mathcal{D}_\alpha)^{\frac{1}{2+\alpha}}\Gamma\left(\frac{1}{2+\alpha}\right)}. \quad (\text{G14})$$

We have written this result in Eq. (57) in the main text.

-
- [1] T. Kühn, T. O. Ihalainen, J. Hyväluoma, N. Dross, S. F. Willman, J. Langowski, M. Vihinen-Ranta and J. Timonen, Protein Diffusion in Mammalian Cell Cytoplasm, *PLoS One*, **6**, e22962 (2011).
- [2] B. P. English, V. Hauryliuk, A. Sanamrad, S. Tankov, N. H Dekker and J. Elf, Single-molecule investigations of the stringent response machinery in living bacterial cells, *Proc. Natl. Acad. Sci. U. S. A.*, **108**, E365 (2011).
- [3] M. Platani, I. Goldberg, A. I. Lamond and J. R. Swedlow, Cajal body dynamics and association with chromatin are ATP-dependent, *Nat. Cell Biol.*, **4**, 502 (2002).
- [4] P. Lançon, G. Batrouni, L. Lobry and N. Ostrowsky, Drift without flux: Brownian walker with a space-dependent diffusion coefficient, *Eur. Phys. Lett.*, **54**, 28 (2001).
- [5] M. Yanga and M. Ripoll, Drift velocity in non-isothermal inhomogeneous systems, *J. Chem. Phys.*, **136**, 204508 (2012).
- [6] J. J. Erik Maris, D. Fu, F. Meirer and B. M. Weckhuysen, Single-molecule observation of diffusion and catalysis in nanoporous solids, *Adsorption*, **27**, 423 (2021).
- [7] J. Mittal, T. M. Truskett, J. R. Errington and G. Hummer, Layering and Position-Dependent Diffusive Dynamics of Confined Fluids, *Phys. Rev. Lett.*, **100**, 145901 (2008).
- [8] L. F. Richardson, Atmospheric diffusion shown on a distance-neighbour graph, *Proc. R. Soc. London, Ser. A*, **110**, 709 (1926).
- [9] B. O’Shaughnessy and I. Procaccia, Analytical Solutions for Diffusion on Fractal Objects, *Phys. Rev. Lett.*, **54**, 455 (1985).
- [10] A. G. Cherstvy and R. Metzler, Population splitting, trapping, and non-ergodicity in heterogeneous diffusion processes, *Phys. Chem. Chem. Phys.*, **15**, 20220 (2013).
- [11] A. G. Cherstvy, A. V. Chechkin and R. Metzler, Particle invasion, survival, and non-ergodicity in 2D diffusion processes with space-dependent diffusivity, *Soft Matter*, **10** 1591 (2014).
- [12] N. Leibovich and E. Barkai, Infinite ergodic theory for heterogeneous diffusion processes, *Phys. Rev. E*, **99**, 042138 (2019).
- [13] X. Wang, W. Deng and Y. Chen, Ergodic properties of heterogeneous diffusion processes in a potential well, *J. Chem. Phys.*, **150**, 164121 (2019).
- [14] K. S. Fa and E. K. Lenzi, Anomalous diffusion, solutions and first passage time: influence of diffusion coefficient, *Phys. Rev. E*, **71**, 012101 (2005).
- [15] N. M. Mutothya, Y. Xu, Y. Li and R. Metzler, Characterising stochastic motion in heterogeneous media driven by coloured non-Gaussian noise, *J. Phys. A: Math. Theor.*, **54**, 295002 (2021).
- [16] Y. Xu, X. Liu, Y. Li and R. Metzler R, Heterogeneous diffusion processes and non-ergodicity with Gaussian coloured noise in layered diffusivity landscapes *Phys. Rev. E*, **102**, 062106 (2020).
- [17] N. M. Mutothya, Y. Xu, Y. Li, R. Metzler and N. M. Mutua, First passage dynamics of stochastic motion in

- heterogeneous media driven by correlated white Gaussian and coloured non-Gaussian noises, *J. Phys. Complex.*, **2**, 045012 (2021).
- [18] P. Singh, S. Sabhapandit and A. Kundu, Run-and-tumble particle in inhomogeneous media in one dimension, *J. Stat. Mech.*, 083207 (2020).
- [19] P. Lévy, On certain homogeneous stochastic processes. *Compositio mathematica*, **7**, 283 (1940).
- [20] S. N. Majumdar, J. Randon-Furling, M. J. Kearney and M. Yor, On the time to reach maximum for a variety of constrained Brownian motions, *J. Phys. A: Mathematical and Theoretical*, **41**, 365005 (2008).
- [21] P. Singh and A. Pal, Extremal statistics for stochastic resetting systems, *Phys. Rev. E*, **103**, 052119 (2021).
- [22] F. Mori, S. N. Majumdar and G. Schehr, Distribution of the time of the maximum for stationary processes, *Euro Phys. Lett.*, **135** 30003 (2021).
- [23] G. Schehr and S. N. Majumdar, Exact record and order statistics of random walks via first-passage ideas, in *First-Passage Phenomena and Their Applications*, edited by R. Metzler, G. Oshani, and S. Redner (World Scientific Publishing Co., Singapore, 2014), 226.
- [24] G. Schehr, S. N. Majumdar, A. Comtet and J. Randon-Furling, Exact distribution of the maximal height of p vicious walkers, *Phys. Rev. Lett.*, **101**, 150601, (2008).
- [25] E. Brunet and B. Derrida, Statistics at the tip of a branching random walk and the delay of traveling waves, *EPL*, **87**, 60010 (2009).
- [26] J. Rambeau and G. Schehr, Distribution of the time at which N vicious walkers reach their maximal height, 2011, *Phys. Rev. E*, **83**, 061146.
- [27] E. S. Andersen, On the fluctuations of sums of random variables, *Math. Scand.*, **2**, 195 (1954).
- [28] S. N. Majumdar, A. Rosso and A. Zoia, Time at which the maximum of a random acceleration process is reached. *J. Phys. A: Math. and Th.*, **43**, 115001 (2010).
- [29] T. W. Burkhardt, Semiflexible polymer in the half plane and statistics of the integral of a Brownian curve, *J. Phys. A: Math. Gen.*, **26**, L1157 (1993).
- [30] P. Singh, Random acceleration process under stochastic resetting, *J. Phys. A: Math. Theor.*, **53**, 405005 (2020).
- [31] P. Singh, and A. Kundu, Generalised ‘Arcsine’ laws for run-and-tumble particle in one dimension. *J. Stat. Mech.*, 083205 (2019).
- [32] F. Mori, P. Le Doussal, S. N. Majumdar and G. Schehr, Universal survival probability for a d -dimensional run-and-tumble particle, *Phys. Rev. Lett.*, **124**, 090603 (2020).
- [33] K. J. Wiese, S. N. Majumdar and A. Rosso, Perturbation theory for fractional Brownian motion in presence of absorbing boundaries, *Phys. Rev. E*, **83**, 061141 (2011).
- [34] T. Sadhu, M. Delorme and K. J. Wiese, Generalized arcsine laws for fractional Brownian motion, *Phys. Rev. Lett.*, **120**, 040603 (2018).
- [35] S. N. Majumdar, A. Rosso and A. Zoia, Hitting probability for anomalous diffusion processes, *Phys. Rev. Lett.*, **104**, 020602 (2010).
- [36] G. Schehr and P. Le Doussal, Extreme value statistics from the real space renormalization group: Brownian motion, Bessel processes and continuous time random walks, *J. Stat. Mech.*, P01009 (2010).
- [37] D. S. Dean and S. N. Majumdar, Large deviations of extreme eigenvalues of random matrices, *Phys. Rev. Lett.*, **97**, 160201 (2006).
- [38] S. N. Majumdar and M. Vergassola, Large deviations of the maximum eigenvalue for Wishart and Gaussian random matrices, *Phys. Rev. Lett.*, **102**, 060601 (2009).
- [39] S. N. Majumdar and G. Schehr, Top eigenvalue of a random matrix: large deviations and third order phase transition, *J. Stat. Mech.*, P01012 (2014).
- [40] S. Raychaudhuri, M. Cranston, C. Przybyla and Y. Shapir, Maximal height scaling of kinetically growing surfaces, *Phys. Rev. Lett.*, **87**, 136101 (2001).
- [41] S. N. Majumdar and A. Comtet, Exact maximal height distribution of fluctuating interfaces, *Phys. Rev. Lett.*, **92**, 225501 (2004).
- [42] J. Rambeau, and G. Schehr, Extremal statistics of curved growing interfaces in $1+1$ dimensions, *EPL*, **91**, 60006 (2010).
- [43] S. N. Majumdar, *Real-space condensation in stochastic mass transport models, in Exact Methods in Low-Dimensional Statistical Physics and Quantum Computing: Lecture Notes of the Les Houches Summer School*, Vol. 89, July 2008, edited by J. Jacobsen, S. Ouvry, V. Pasquier, D. Serban, and L. Cugliandolo (Oxford University Press, Oxford, 2010), p. 407.
- [44] A. Guillet, E. Roldán, and F. Jülicher, Extreme-value statistics of stochastic transport processes, *New J. Phys.* **22**, 123038 (2020).
- [45] M. R. Evans and S. N. Majumdar, Condensation and extreme value statistics, *J. Stat. Mech.* (2008) P05004.
- [46] S. N. Majumdar and J. P. Bouchaud, Optimal time to sell a stock in the Black-Scholes model: Comment on ‘Thou Shalt Buy and Hold’, by A. Shiryaev, Z. Xu and X. Y. Zhou, *Quant. Financ.* **8**, 753 (2008).
- [47] Y. V. Fyodorov and J. P. Bouchaud, Freezing and extreme-value statistics in a random energy model with logarithmically correlated potential, *J. Phys. A: Math. Theor.* **41**, 372001 (2008).
- [48] A. Bar, S. N. Majumdar, G. Schehr, and D. Mukamel, Exact extreme-value statistics at mixed-order transitions, *Phys. Rev. E* **93**, 052130 (2016).
- [49] M. Höll, W. Wang, and E. Barkai, Extreme value theory for constrained physical systems, *Phys. Rev. E* **102**, 042141 (2020).
- [50] L. Frachebourg, I. Ispolatov, and P. L. Krapivsky, Extremal properties of random systems, *Phys. Rev. E* **52**, R5727 (1995).
- [51] C. Godreche, S. N. Majumdar, and G. Schehr, Longest Excursion of Stochastic Processes in Nonequilibrium Systems, *Phys. Rev. Lett.* **102**, 240602 (2009).
- [52] M. R. Leadbetter, G. Lindgren, and H. Rootzén, *Extremes and Related Properties of Random Sequences and Processes* (Springer Science & Business Media, New York, 1983).
- [53] R. A. Fisher and L. H. C. Tippett, Limiting forms of the frequency distribution of the largest or smallest member of a sample, *Math. Proc. Camb. Philos. Soc.* **24**, 180 (1928).
- [54] B. Gnedenko, Sur La Distribution Limite Du Terme Maximum D’Une Série Aléatoire, *Ann. Math.* **44**, 423 (1943).
- [55] E. J. Gumbel, *Statistics of Extremes* (Dover, New York, 1958).
- [56] J. Y. Fortin and M. Clusel, Applications of extreme value statistics in physics, *J. Phys. A: Math. Theor.* **48**, 183001 (2015).
- [57] S. Albeverio, V. Jentsch, and H. Kantz (eds.), *Extreme Events in Nature and Society* (Springer Science & Busi-

- ness Media, Berlin, Germany, 2006).
- [58] S. N. Majumdar, A. Pal, and G. Schehr, Extreme value statistics of correlated random variables: A pedagogical review, *Phys. Rep.* **840**, 1 (2020).
- [59] J. P. Bouchaud and M. Mézard, Universality classes for extreme-value statistics, *J. Phys. A: Math. Gen.* **30**, 7997 (1997).
- [60] S. Sabhapandit, Extremes and records, arXiv:1907.00944.
- [61] S. N. Majumdar, Universal first-passage properties of discrete-time random walks and Lévy flights on a line: Statistics of the global maximum and records, *Physica A* **389**, 4299 (2010).
- [62] E. Dumonteil, S. N. Majumdar, A. Rosso, and A. Zoia, Spatial extent of an outbreak in animal epidemics, *Proc. Natl. Acad. Sci. USA* **110**, 4239 (2013).
- [63] S. N. Majumdar and P. L. Krapivsky, Extreme value statistics and traveling fronts: Application to computer science, *Phys. Rev. E* **65**, 036127 (2002).
- [64] S. N. Majumdar, Traveling front solutions to directed diffusion-limited aggregation, digital search trees, and the Lempel-Ziv data compression algorithm, *Phys. Rev. E* **68**, 026103 (2003).
- [65] P. L. Krapivsky and S. N. Majumdar, Traveling Waves, Front Selection, and Exact Nontrivial Exponents in a Random Fragmentation Problem, *Phys. Rev. Lett.* **85**, 5492 (2000).
- [66] J. Randon-Furling, S. N. Majumdar, and A. Comtet, Convex Hull of N Planar Brownian Motions: Exact Results and an Application to Ecology, *Phys. Rev. Lett.* **103**, 140602 (2009).
- [67] F. Mori, S. N. Majumdar, and G. Schehr, Time Between the Maximum and the Minimum of a Stochastic Process, *Phys. Rev. Lett.* **123**, 200201 (2019).
- [68] F. Mori, S. N. Majumdar, and G. Schehr, Distribution of the time between maximum and minimum of random walks, *Phys. Rev. E* **101**, 052111 (2020).
- [69] S. N. Majumdar, Brownian Functionals in Physics and Computer Science, *Current Science* **89** 2076 (2005).
- [70] A. Dhar and S. N. Majumdar, Residence time distribution for a class of Gaussian Markov processes, *Phys. Rev. E* **59** 6413 (1999).
- [71] S. N. Majumdar and D. S. Dean, Exact occupation time distribution in a non-Markovian sequence and its relation to spin glass models, *Phys. Rev. E* **66** 041102 (2002).
- [72] S. N. Majumdar and A. Comtet, Local and the Occupation Time of a Particle Diffusing in a Random Medium, *Phys. Rev. Lett.* **89** 060601 (2002).
- [73] S. Sabhapandit, S. N. Majumdar and A. Comtet, Statistical Properties of Functionals of the Paths of a Particle Diffusing in a One-Dimensional Random Potential, *Phys. Rev. E* **73** 051102 (2006).
- [74] F. den Hollander, S. N. Majumdar, J. M. Meylahn and H. Touchette, Properties of additive functionals of Brownian motion with resetting, *J. Phys. A: Math. Theor.*, **52**, 175001 (2019).
- [75] A. Comtet, F. Cornu and G. Schehr, Last-Passage Time for Linear Diffusions and Application to the Emptying Time of a Box, *J. Stat. Phys.*, **181** 1565 (2020).
- [76] A. Comtet, J. Desbois, Brownian motion in wedges, last passage time and the second arc-sine law, *J. Phys. A*, **36**, L255 (2003).
- [77] H. Boutcheng, T. Bouetou, T. W. Burkhardt, A. Rosso, A. Zoia and K. T. Crepin, Occupation time statistics of the random acceleration model, *J. Stat. Mech.*, (2016) 053213.
- [78] S. Carmi, L. Turgeman and E. Barkai, On Distributions of Functionals of Anomalous Diffusion Paths, *J. Stat. Phys.* **141**, 1071 (2010).
- [79] P. C. Bressloff, Occupation time of a run-and-tumble particle with resetting, *Phys. Rev. E*, **102**, 042135 (2020).
- [80] D. Charles and W. Rosemarie, The arcsine law and the treasury bill futures market, *Financial Analysts Journal* **36** 71 (1980).
- [81] A. N. Shiryaev, Quickest Detection Problems in the Technical Analysis of the Financial Data, In *Mathematical Finance Bachelier Congress 2000*, Springer, New York, 487 (2002).
- [82] A. Baldassarri, J. P. Bouchaud, I. Dornic and C. Godrèche, Statistics of persistent events: An exactly soluble model, *Phys. Rev. E* **59**, R20(R) (1999).
- [83] C. Godrèche and J. M. Luck, Statistics of the occupation time of renewal processes, *J. Stat. Phys.*, **104** 489 (2001).
- [84] S. Burov and E. Barkai, Residence Time Statistics for N Renewal Processes, *Phys. Rev. Lett.* **107** 170601 (2011).
- [85] Y. Kasahara, Limit Theorems of Occupation Times for Markov Processes, *Publ. RIMS, Kyoto Univ.*, **12** 801 (1977).
- [86] J. Lamperti, An Occupation Time Theorem for A Class of Stochastic Processes, *Trans. Amer. Math. Soc.*, **88** 380 (1958).
- [87] A. C. Barato, E. Roldán, I. A. Martínez and S. Pigolotti, Arcsine Laws in Stochastic Thermodynamics, *Phys. Rev. Lett.* **121** 090601 (2018).
- [88] R. Dey, A. Kundu, B. Das and A. Banerjee, Experimental verification of Arcsine laws in mesoscopic non-equilibrium and active systems, arXiv:2104.00127.
- [89] N. G. van Kampen, Itô versus Stratonovich, *J. Stat. Phys.* **24** 175 (1981).
- [90] A. W. C. Lau and T. C. Lubensky, State-dependent diffusion: Thermodynamic consistency and its path integral formulation, *Phys. Rev. E* **76**, 011123 (2007).
- [91] M. Kac, On distributions of certain Wiener functionals, *Trans. Am. Math. Soc.* **65**, 1 (1949).
- [92] S. Redner, *A Guide to First-Passage Processes* (Cambridge University Press, Cambridge, England, 2001).
- [93] W. Feller, *An Introduction to Probability Theory and its Applications* (New York: Wiley, 1968).